



Escola Politècnica Superior
de Castelldefels

UNIVERSITAT POLITÈCNICA DE CATALUNYA

TREBALL DE FI DE CARRERA

TÍTULO: Development and analysis of Laser Scanner data

DEGREE: Technical Telecommunication Engineering

Speciality: Telematics

AUTHOR: Emma Riera Wilson

DIRECTOR: Michele Crosetto

SUPERVISOR: Jaume Piera Fernández

DATE: 18th February 2008

TÍTULO: Development and analysis of Laser Scanner data

DEGREE: Technical Telecommunication Engineering

Speciality: Telematics

AUTHOR: Emma Riera Wilson

DIRECTOR: Michele Crosetto

SUPERVISOR: Jaume Piera Fernández

DATE: 18th February 2008

Overview

Terrestrial Laser Scanning offers an alternative to traditional survey techniques and consists of high speed data capture. This technique is very recent and is still being studied.

The aim of this project is to study the capabilities of Terrestrial Laser Scanners for Land Deformation Monitoring.

This document firstly reviews the basic functioning of Terrestrial Laser Scanning technique and device. Furthermore it describes in detail the experimental work carried out at the Institute of Geomatics (IG).

TÍTOL: Elaboració i anàlisi de dades de Laser Scanner

DEGREE: Enginyeria Tècnica de Telecomunicació

Especialitat: Telemàtica

AUTOR: Emma Riera Wilson

DIRECTOR: Michele Crosetto

SUPERVISOR: Jaume Piera Fernández

DATA: 18 de febrer de 2008

Resum

Terrestrial Laser Scanner ofereix una alternativa per tècniques tradicionals de medició que consisteix en medició de dades a gran velocitat. Aquesta tècnica és molt jove i encara s'està estudiant.

L'objectiu d'aquest projecte és estudiar les capacitats de Terrestrial Laser Scanner per a Deformacions en el terreny.

Aquest document primer estudia el funcionament bàsic de la tècnica i l'aparell de Terrestrial Laser Scanner. Després descriu amb detall el treball experimental fet a l'Institut de Geomàtica (IG).

ÍNDIX

INTRODUCTION	1
CHAPTER 1: WORKING PRINCIPLES	2
1.1.Instrument description	2
1.2.TLS classification	5
1.2.1.Distance measurement principle	5
1.2.1.1.Time of Flight	5
1.2.1.2.Phase Difference	6
1.2.1.3Optical Triangulation	7
1.2.2.Deflection of laser beam	9
1.2.2.1.Camera view	9
1.2.2.2.Panoramic view	9
1.2.2.3.Hybrid view	10
1.3.Classification by technical properties	10
CHAPTER 2: DATA PROCESSING.....	11
2.1.Data processing	11
2.1.1.Data acquisition	11
2.1.2.Data treatment	12
2.1.3.Data visualization	13
2.2.Influence of the characteristics of the object (Reflectivity)	13
2.3.Influence of environmental conditions	15
2.4.TLS applications	16
CHAPTER 3: DATA ANALYSIS	20
3.1.Available experimental data.....	20
3.1.1.Castellfollit village	20
3.1.2.Experiment at the Institute of Geomatics	21
3.1.3.Formigal village	23
3.2.Data Analysis.....	24
3.3.Matching	24
3.3.1.Least Squares 3D surface matching	24
3.3.2.Matching analysis	25
3.3.3.Precision analysis	29
3.4.Residuals vs Photograph	33
3.5.Incidence Angle vs Residuals	36
3.6.Analysis of Standard Deviation measurements.....	40
3.6.1.Use of Standard Deviation value	44
3.7.Study of the influence of the characteristics of the object.	49
CONCLUSIONS	53

BIBLIOGRAPHY	54
ANNEX	56

INTRODUCTION

The aim of this document is to study the capabilities of TLS technology to be used for Land Deformation Monitoring. TLS technology is based on Light Distance and Ranging (LiDAR) and is also referred to as ground-based LiDAR or tripod LiDAR.

*“**LIDAR** (Light Detection and Ranging; or Laser Imaging Detection and Ranging) is a technology that determines the distance to an object or surface using laser pulses. Like the similar radar technology, which uses radio waves instead of light, the range to an object is determined by measuring the time delay between transmission of a pulse and detection of the reflected signal. LIDAR technology has application in geology, seismology, remote sensing and atmospheric physics” [14].*

The primary capability of TLS is the generation of high resolution 3-dimensional maps and images of objects over scales of metres to kilometres with centimetre or under centimetre precision. This allows for high accuracy mapping as well as the determination of surface changes over time via repeated measurements.

The document is divided into three chapters:

-WORKING PRINCIPLES: Introduction to the main functioning and types of TLS devices.

-DATA: Deals with the collection and treatment of data obtained from TLS devices and it also explains the influence depending on the characteristics of the object.

-EXPERIMENTAL PART: This is the most important part of the document. In this chapter different experiments are carried out to study the data obtained from TLS devices, especially for Land Deformation Monitoring.

CHAPTER 1 : WORKING PRINCIPLES

Terrestrial Laser Scanning (TLS) offers an alternative to traditional survey techniques and consists of high speed data capture. Terrestrial Laser Scanning works like ordinary radars, except these systems send out narrow pulses or beams of light rather than broad radio waves. A receiver system processes the returning light to calculate the point cloud corresponding to the measured area.

TLS systems are an active noncontact range-finding device. The basic principle of these types of devices is to project an optical signal onto an object and then process the reflected or scattered signal to determine the distance. For each reflected signal, scanners collect four measurements:

- Two angles (horizontal and vertical)
- Distance
- Intensity

With the two angles and the distance the TLS obtains a polar coordinate for every measured point in the target. Once these polar coordinates have been measured they are immediately transformed into a local 3D Cartesian system (x,y,z). Finally, these internal coordinates are treated and transformed into an external coordinate system by specific software.

1.1. Instrument Description

TLSs are high precision systems, capable of working in most real world environments under a variety of conditions. In order to work properly and to have an accurate result, ground-based Lidars must be placed in a way that will guarantee no movements will occur during the measurements. The most reliable way is to mount the Lidar on a tripod, ensuring constant position and orientation in short and middle time-length measurements. Whereas, for long time monitoring a more stable and solid platform is recommended.

TLSs use tacheometric measurements [2], which consist of the combination of measured distances to the target and the angles from the device. The principle can be seen in image 1.1:

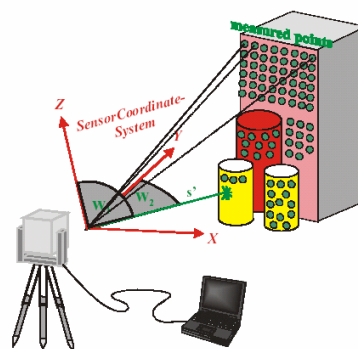


Image 1.1 - Tacheometric Laser Scanning principle

The laser scanner range finder only detects the distance of one point at a time in its view direction. Thus, the scanner scans its entire field of view (FoV), one point at a time, by changing the laser's view direction to scan different points. The view direction of the laser scanner can be changed by either rotating the device itself, or by using a system of rotating mirrors. The latter method is the most used, because mirrors are much lighter and can be rotated much faster and with a greater accuracy.

The laser Scanner calculates an oblique distance (s') and two orthogonal angles (w_1 and w_2) for every measured point in the target surface. With these parameters the TLS defines the position of every point in the space in a polar coordinate system. The measured angles correspond to the horizontal direction (w_2) and the vertical direction (w_1). These polar coordinates are transformed into an internally defined Cartesian system (x,y,z). The reference of this internal coordinate system is the TLS geometric rotation centre, this point is considered as the zero point (0,0,0).

Image 1.2 is a picture of a type of TLS:

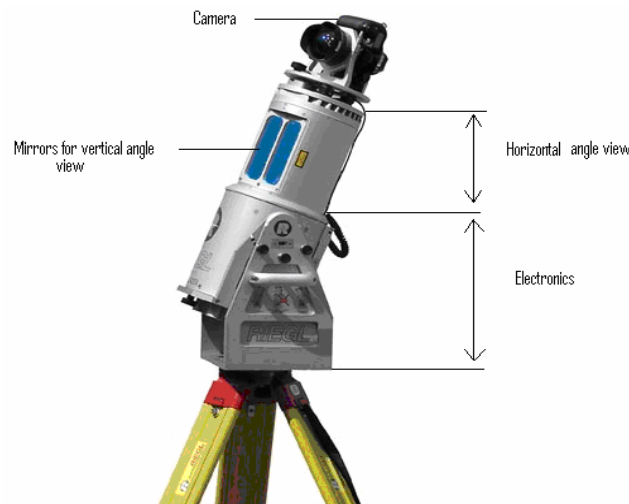


Image 1.2 - Terrestrial Laser Scanner. RIEGL LMS-Z420i [15]

The horizontal scan, also called “frame scan”, is the part responsible for measuring the angle in the horizontal direction (w_2). Image 1.2 shows the rotating optical head of the instrument with two vertical windows. It is mounted on a cylinder which connects it to the base tripod. The horizontal scan can have a FoV from 40° up to 360° , depending on the rotation of the complete optical head.

Inside the windows of the rotating head there are two mirrors which are responsible for scanning in the vertical direction, also called “line scan”. The mirrors in the rotating head are polygonal with a number of reflective surfaces. The mirrors can be *rotating* or *oscillating* depending on the size of the angles it is measuring:

- For high scanning rates and a large vertical scan angle, the *polygonal mirror rotates* continuously at an adjustable speed.
- For slow scanning rates and small scanning angles, the *polygonal mirrors oscillate* linearly up and down.

The vertical scan can have a FoV from 40° up to 310° . The FoV is limited to 310° because of the support that holds the Lidar.

Regarding the part that calculates the distance to the target, there are different possible mechanisms that can be used. These mechanisms are explained in the next point.

Once the angles and the distance for each point in the point cloud have been measured, they are monitored and recorded with high precision and then transmitted to the storage device. As explained before, these polar coordinates are then transformed into an internal Cartesian coordinate system (x,y,z) , which can be later georeferenced into an external co-ordinate system (X,Y,Z) as is shown in image 1.3:

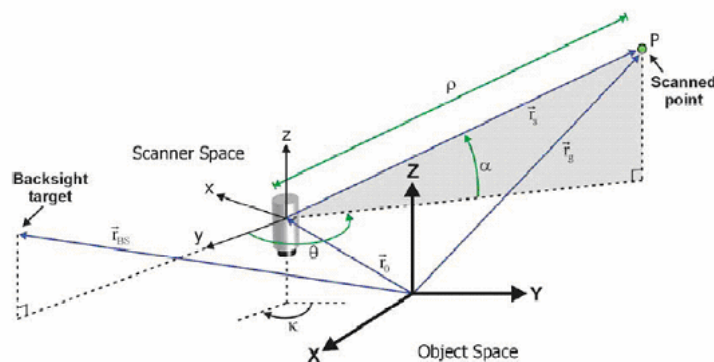


Image 1.3 - Co-ordinate Systems [9]

In addition, the *intensity* (i) of the returning distance signal for each point is also stored. The intensity is a measurement of the received energy for each point. The intensity is often called the fourth dimension and it is very useful for the visualization of the target, especially in dense and complex point clouds.

To sum up, the Laser scanner creates a point cloud where each point is determined by position (x,y,z) and intensity (i).

To add information, digital images can be taken during the data capture. A digital camera may be fixed to the TLS or may be used independently. Photographs give information about the colour and the texture of the object. This information is very useful in measurements where there is, for example, a lot of vegetation, which introduces noise. Colour information can help remove the mentioned noise.

1.2. TLS classification

It is difficult to classify TLSs because most of the available laser scanners are not well specified, but there are several possible ways of doing this classification:

- Distance measurement principle
- Deflection of the laser beam
- Other technical specifications

1.2.1. Distance measurement principle

Mainly, the distance measurement system correlates to both the range and the resulting accuracy of the system. Therefore, this implies a categorization by range as well as by accuracy. The accuracy of the distance measurements depends on the intensity of the reflected laser light and therefore directly on the reflectivity of the object. We can find three basic technologies for distance measurements:

- Time of Flight (TOF) (pulsed method)
- Phase measurement system (Interferometry)
- Optical triangulation approach.

1.2.1.1. Time of Flight

The most popular measurement system for laser scanning is the Time of Flight (TOF) [16][10]. This system uses the time it takes for a pulse of energy to travel from its transmitter to the observed object and back. Light is used as the energy source, so the relevant parameter involved is the speed of light, roughly 0.3m/ns. Using this parameter we can calculate how far a returning light photon has travelled to and from an object:

- The Laser scanner generates the optical pulse.
- The pulse is reflected off an observed object and returns to the laser scanner.
- A high-speed counter in the laser scanner measures the time of flight from the start pulse to the return pulse.
- Finally, the distance is calculated using the following formula:

$$d = \frac{c \cdot TOF}{2} \quad (1.1)$$

In the above formula the speed of light (c) must be multiplied by the time light takes to travel the distance. In this case, the measured time (TOF) represents twice the distance; this is why it is divided by 2.

Time of flight range finders are capable of operating over long distances, in the order of a kilometre. These scanners are thus suitable for scanning large structures like buildings or geographic features. The disadvantage of TOF systems is their lack of accuracy. Due to the high speed of light, timing the round-trip-time is difficult and accuracy of the distance is relatively low, in the order of millimetres. The further away the target, the less the accuracy.

1.2.1.2. Phase difference (Interferometry)

The phase measurement system [3][10] uses one or two long waves to modulate the laser radiation. The phase difference between the emitted signal and the received one is used to compute the range. To be more exact, the optical power is modulated with a constant frequency. A sine wave of frequency (F), generated by the main oscillator, modulates the continuous current (dc) of the laser diode. After reflection from the target, a photodiode collects a part of the laser beam, and then the distance is deduced from the phase difference between the photoelectric current and the modulated emitted signal:

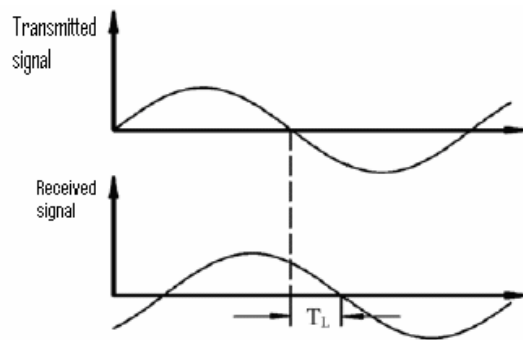


Image 1.4 – Phase difference measurement

$$d = \frac{1}{2} c \frac{\Delta\varphi}{2\pi} f \quad (1.2)$$

$$\Delta\varphi = 2\pi f \Delta t \quad (1.3)$$

Where c is the speed of light and Δt is the TOF.

Distance measurement by the phase technique is a good method to obtain an accuracy of some millimetres for ranges of up to a hundred metres. It is suitable for indoor environments.

1.2.1.3. Optical Triangulation

The Optical triangulation system [17][10] uses a laser light source, a lens and a photodetector to calculate the distance to an object. This measurement principle is called Optical Triangulation system because the laser dot, the photodetector and the laser emitter form a triangle. The geometry of this system is illustrated in image 1.5:

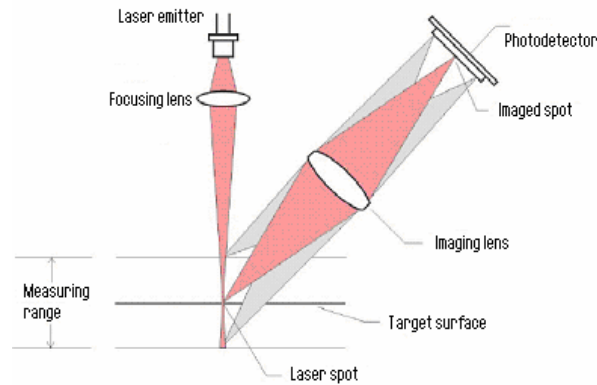


Image 1.5 – Optical triangulation

A Laser is used to generate a focused beam of light that is projected onto a target surface. A lens captures the scattered light and focuses it onto a photodetector. Depending on the distance to the target, the laser dot strikes at a different place in the photodetector's FoV.

The necessary parameters to determine the size and shape of the triangle are the following:

- x : distance between the photodetector and the laser emitter.
- α : the angle of the laser emitter.
- θ : the angle of the photodetector. This angle is calculated looking at the location of the laser dot in the photodetector.
- β : angle of incidence.
- d : distance from the target to the TLS.

In image 1.6 this can be seen:

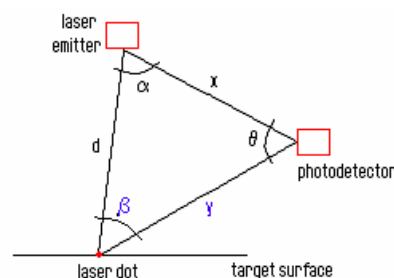


Image 1.6 – Geometry of Optical Triangulation

The distance (d) is calculated using trigonometry. The steps to calculate d are the following:

- First it calculates the angle of incidence β :

$$\beta = 180^\circ - \alpha - \theta \quad (1.3)$$

- Then it calculates d using the sinus theorem:

$$d = \frac{x \sin \theta}{\sin \beta} \quad (1.4)$$

The most important component in the optical triangulation system is the sensor (photodetector). There are two types of sensors depending on the application of the measurement:

- PSD (Position Sensitive Detector) only determines the position of the measured spot and its total intensity, so they are suitable for devices that measure small ranges.
- CCD (Charged Coupled Device) can be used to determine the shape and intensity distribution of the light spot on the photodetector, because they have a better geometric stability.

Triangulation systems are the complete opposite of TOF systems. They have a limited range of some metres, but their accuracy is relatively high, on the order of tens of micrometres.

In the following table we classify the TLS depending on the measurement principle explained above:

Table 2.1. TLS Classification depending on the measurement principle.

Measurement system	Range [m]	Range accuracy [mm]	Manufacturers (examples)
Time of flight	~ 1000	> 10	Mensi, Riegl, Cyra, Callidus
Phase measurement	< 100	< 10	Zoller+Froehlich, IQSun
Optical triangulation, Laser radar	< 10	< 1	Minolta, Leica

1.2.2. Deflection of laser beam

If TLSs are classified depending on the deflection of the laser beam the following types are possible [2][10]:

- Camera view
- Panoramic view
- Hybrid view

1.2.2.1. Camera view

A camera view field is achieved by using two synchronised mirrors, one for horizontal beam deflection and the other for vertical beam deflection. The benefit of this technology is that both mirrors can be positioned individually and a very high accuracy with angular measurements can be achieved. The disadvantage of this technology is that the field of view is limited to a camera view, $60^{\circ} \times 60^{\circ}$. This type is mainly designed for outdoor purposes. These types of instruments are rapidly disappearing, because the field of view is very limited compared to the panoramic view instruments.

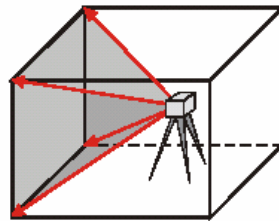


Image1. 7 – Camera view

1.2.2.2. Panoramic view

A panoramic view is achieved by a single rotating mirror that simultaneously rotates the system by the centre axis, vertically and horizontally. The advantage of this technique is that it leads to an easy and quick scanning, as the scene to be modelled has to be surveyed only from a few locations, surveying the scene in a very short time. This type is designed for indoor purposes. The FoV is only limited by the support that holds the TLS.

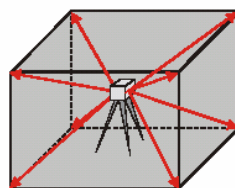


Image 1.8 – Panoramic view

1.2.2.3. Hybrid view

A Hybrid view Scanner, as its name reveals, is a combination between the two types explained before. In this case, we have a rotating axis without restrictions and the other rotating axis is limited due to the mirrors. Normally a monitored scanhead movement is allowed in the horizontal axis.

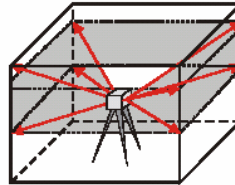


Image 1.9 – Hybrid view

1.3. Classification by technical properties

Finally, to finish the TLS classification, there are more technical specifications that indicate exactly the possibility and the use we can give the Laser:

- Scanning speed, sampling rate of laser measurement system
- Spatial resolution (number of points scanned in field of view)
- Combination with other devices, mounted on the laser scanner (GPS, camera...)

CHAPTER 2. DATA PROCESSING

The following section deals with the collection and treatment of data from TLS instruments. It goes on to explain the effect of measuring different types of target surfaces while scanning, commenting on the effects of texture, colour and orientation based on information extracted from several studies carried out by others.

2.1. Data processing

It is a well known fact to people in the field that there are different types of TLS which are designed and developed for specific tasks. However, data processing is treated in a very similar way for all TLSs [2]. In general, each surveying task can be divided into three major steps:

- Data acquisition
- Data treatment
- Data visualization

2.1.1. Data acquisition

The first step to process data is data acquisition, which consists of measuring the scene with a TLS to obtain the data. The procedure to obtain the mentioned data is also divided into several steps.

Firstly, the area of interest is scanned once or several times. To ensure a full record of the target and to avoid holes in the obtained data, scans from different points of view are recommended. Also various scans in the same position can be used to contrast that the data has been scanned correctly, verifying the precision of this data.

Once data has been scanned a point cloud is obtained, where each point represents a 3D coordinate (xyz) of the situation of the object and the intensity of the reflected signal for each point.

Finally, all the different scans (point clouds) of the same area are fused in a global one. This procedure involves the matching of the different point clouds. *Matching* is a procedure that consists on finding each correspondent point in two different acquisitions to match both acquisitions. There are two techniques for matching:

- Point based Technique: this is the most precise method, because it uses known shared points from the different scans to carry out the matching.
- Area based Technique: this method uses natural structures and is enabled by the existence of matching algorithms like the *Iterative Closest Point (ICP)* method and its many variants. In its most basic form, the

reference point cloud is modelled by triangulation. The other point cloud is transformed to best fit the surface, such that the sum of distances between its points and the surface model is minimised. These algorithms perform best when there is a large overlap and the surface is rough and not smooth. The problem with planar surfaces is that the surface is very homogeneous in all its points and this can cause errors during matching.

Data acquisition is a very fast and easy procedure for present-day systems. The main reasons are that data capture is automated and modern TLS allow a wide Field of view that permits modelling the whole scene from only a few locations.

2.1.2. Data treatment

Once the raw data have been collected they must be treated. Before treating data the quality of the measurement must be looked at. The manufacturers give detailed technical information on their systems, but if a certain quality of measurement is needed, the precision of the 3D-coordinates must be looked at.

The judgment of the quality of the measurements cannot be realized looking at single points (Point based Technique). With TLS the quality measurement has to be realized using groups of points (Area based Technique). A Point based technique cannot be used by TLS because Laser Scanners do not have a telescope for collimation, then it is difficult to measure the exact same point in each observation. The point will be calculated in each observation inside the area of the laser beam diameter. So, the smaller the laser beam diameter, the higher the precision. As mentioned before, an area based technique must be used to solve the problem. This technique extracts groups of points from the laser scanned data.

The scanned point clouds can contain perturbations. These perturbations are caused by wrong points or data voids which can be misinterpreted while examining the different point clouds. These “wrong points” can be caused by:

- Reflexions from temporary obstructions like vehicles, animals or people passing the scene during the scan.
- Total reflexions from the object that can cause either data voids (no information) or virtual objects.

Data voids should be minimised during data acquisition through the selection of appropriate scanning positions and minimising temporary obstructions to the scanner during operation. Data voids due to the occlusion to the line of sight can normally only be eliminated by using multiple scans.

To help eliminate wrong points due to total reflexions a combination of scanned data with digital images is recommended. As mentioned before, the information of colour and texture from digital photographs helps to separate good data from noise or wrong points.

The treatment of data is still a time consuming process. The current bottleneck in TLS data process is the extraction of desired information from the point cloud. This is due to the need of human work for it.

2.1.3. Data visualization

One of the advantages of using point clouds is the visualization of the measured scenes or objects. This view can usually be generated from any direction and with any zoom rate. This visualization can be carried out in different ways:

- Point clouds in a 3D-projection, with a colour or greyscale-coded intensity representation, are often used as a first visual check of the acquired data.
- Point clouds can also be combined with derived geometrical elements.
- Ortho-Photos are realized by the fusion of digital images and the registered point clouds.

2.2. Influence of the characteristics of the object (Reflectivity)

Distance measurement precision is one of the most important features of TLS. It is predominated by both distance measurement systems (TOF, triangulation and phase measurement) and by technical details of the instrument in question. Each system has its own measurement accuracy.

An influence of surface properties like colour, material and shape can be observed. The accuracy of distance measurements depends mainly on the intensity of the reflected laser light and therefore directly on the reflectivity of the object surface. The reflectivity depends on the angle of incidence and the surface properties. The influence of environmental conditions is commented in section 2.3.

Study of colour and surface parameters made by [5] indicate that they are directly connected to the reflectivity factor. This study was carried out in a prepared indoor scenario, so it is rather a specific effect, we do not know exactly its impact in general. This reflectivity factor is presented in percentage values and is equal to the following relation of energy:

Reflectivity factor= received energy from the target / emitted energy from the TLS * 100

The main rule is that the bigger the reflectivity factor, the smaller the Standard Deviation value of the point cloud.

In [5] a selection of coloured sheets were scanned with Mensi GS100 in order to find out the reflectivity factor value depending on the colour. The results gave a scale that classifies the colours and the obtained reflectivity factor. A scale from 0 to 100, where 0 corresponds to the colour black and 100 to the colour white. The scale can be observed in image 2.1:

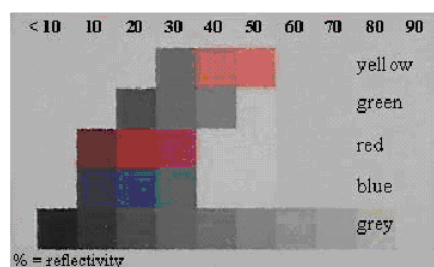


Image 2.1 – Reflectivity factor scale

As can be seen, dark colours have a lower reflectivity factor than light colours, so higher Standard Deviations will be registered with the former and lower distances with the latter. The effect can be visualized in image 2.2:

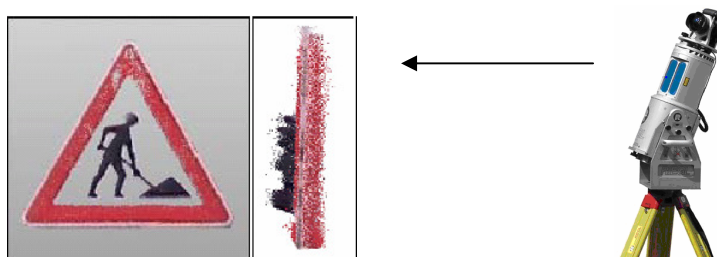


Image 2.2 – Example of reflectivity factor [5].

Image 2.2 represents the front and side views of the point cloud obtained from measuring a traffic sign. The side view must be visualized from the right hand side because it is where the TLS was located while measuring. On this target we can only visualize three colours, black, red and white. As was mentioned before, black has the lowest reflectivity factor value, so it should be the colour with the highest Standard Deviation. In the image we can observe that black points are the furthest away from the TLS whereas white points cannot be visualized because white is a very reflective surface. Highly reflective objects may saturate some laser detectors, while the return signal from low-reflectivity objects may occasionally be too weak to register as valid.

Regarding the texture of the target, matt and rough surfaces have got a lower reflectivity factor than shiny and smooth ones.

Another parameter that should be considered is the angle of incidence. The angle of incidence is directly connected to the shape of the target. In general, the bigger the angle of incidence, the smaller the returning energy to the instrument. This is why it is important to choose the best possible position of the TLS in relation to the target. The best position is to have the surface of the target perpendicular to the TLS beam, because then there is a good reflectivity and a small incidence angle is obtained. The general rule is that the more parallel the surface of the target from the TLS the bigger the angle of incidence. This is also why rough surfaces have got a lower reflectivity factor than smooth

ones. This is due to the heterogeneous nature of rough surfaces which will obviously have less points positioned perpendicularly to the TLS than the smooth homogeneous surfaces.

In areas where the surface has a round shape serious errors can occur. This effect is demonstrated in image 2.3 where a sphere was scanned.

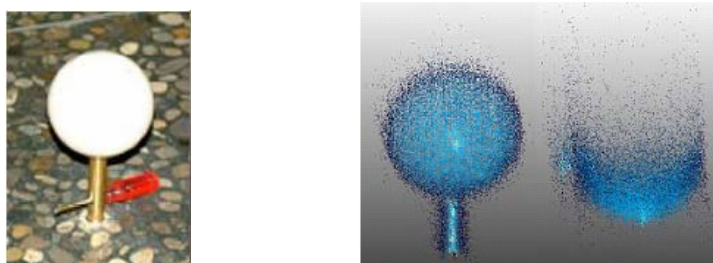


Image 2.3 –Photograph of a sphere (left). Point cloud of a sphere as front view (middle) and as a view from above (right) [5].

Image 2.3 represents the front view and view from above of the point cloud obtained from measuring a sphere. As can be observed, there is a higher dispersion of the points the nearer it gets to the outline. This is due to the incidence angle, because the nearer to the outline of the round object, the bigger the incidence angle, causing a higher dispersion of the data.

The measurement accuracy or standard deviation can be improved by increasing the number of distance measurement shots. By increasing the shots redundancy is obtained. However, multiple measurements can also cause negative effects. For rough and for dark surfaces a multiple measurement leads to a reduction of the dispersion. In contrast, for smooth surfaces and for a 0° angle of incidence, multiple measurements frequently lead to a wrong result of measurement and to a high dispersion of the points.

2.3. Influence of environmental conditions

The effect of environmental conditions [13] is a possible effect that must be looked into because most surveys carried out by TLS are realized in outdoor environments.

On the one hand, TLSs are not affected by the following environmental conditions:

- *Illumination*: TLSs use an “active illumination” technique that, unlike photography, does not depend on ambient illumination, so TLSs can work during the day or at night.
- *Temperature or temperature variation*.
- *Background noise*.

On the other hand, there are some conditions that affect TLS measurements:

- *Sunlight and reflections*: a strong sunlight reflection off a highly reflective target may saturate a receiver, producing an invalid or less accurate reading. However, laser measurements are not usually affected by other reflections
- *Dust and vapour*: laser measurements can also be weakened by interacting with dust and vapour particles, which scatter the laser beam and the signal returning from the target.
- *Radiation*: TLS devices determine baseline radiation levels to ensure that it does not interfere with the measurements.

2.4. TLS applications

TLS is a young and recent instrument; therefore the number of applications is still rising. TLSs can be used for the following applications [13]:

- Architecture and cultural heritage

Structural surveying is an important step in urban design, from construction through to historical preservation. Using traditional methods, structural surveying is time-intensive and costly undertaking. Laser systems provide the means to reduce the time and cost significantly. Since the introduction of laser scanning technology there has been a misconception that the technology is not suitable for structural surveys due to accuracy limitations. But really, the strength of a laser scanner is not in its single shot precision but in its ability to sample the target area.

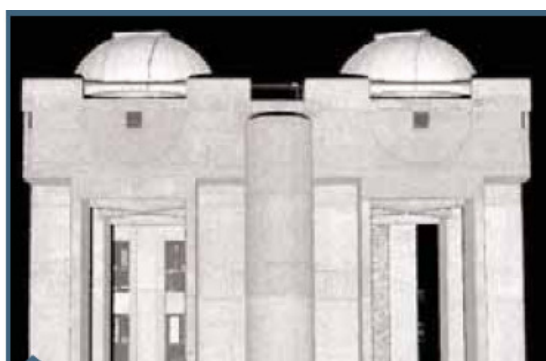


Image 2.4 – Point cloud of a building.

- Mine Planning and Tunnel surveying

Data collection for current methods of open mine volume calculations and tunnel surveying are long and often dangerous. Single point collection with a total station and pole man along various slopes and faces is labour intensive, costly, and most important, dangerous. Therefore, measurements can be collected much more effectively and with no risk using Terrestrial Laser Scanner technology.



Image 2.5 - Point cloud of a tunnel section

- Topographical surveys

In the past, topographical surveys were dominated by total stations, theodolites and, more recently, GPS systems. However, these traditional methods record a limited amount of measured points compared to Terrestrial Laser Scanner technologies. Additionally, these methods are labour-intensive, costly and inconvenient. In many cases, measurements with other devices rather than TLS have a lack of key information or vital points that make it more difficult to obtain good measurement results.

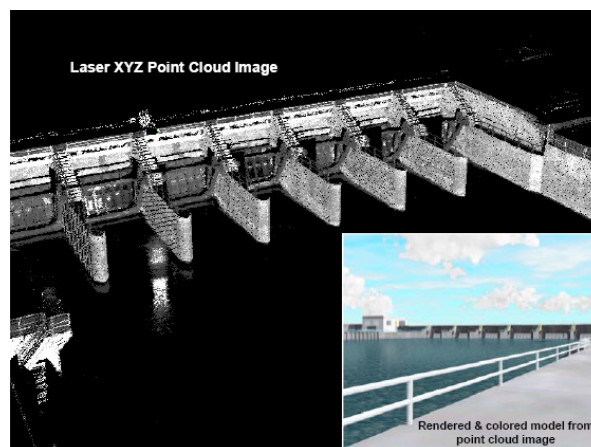


Image 2.6 – Point cloud of downstream gate structures.

- Object monitoring

Modern surveying instruments, such as Total Stations and GPS receivers, have made this task easier and less time-consuming than traditional methods, but still do not offer the required point spacing to deliver a comprehensive surface analysis. Three dimensional laser imaging is the latest technology to be used in this essential monitoring process. Instead of using several dozen “target” points to monitor movement, users can only rely on a “point cloud” consisting of hundreds of thousands or even millions of points to represent the structure being measured.

- Forensic Survey: Accident Reconstruction

In the wake of an accident, experts are employed to aid in the reconstruction of the events that led to it. These experts provide vital functions, ranging from the identification of contributing factors to present in a court of law. Accurate documentation of the "crash environment" is vital for these experts. To determine the most probable scenario leading to the accident, physical elements such as skid marks, road settings ,etcetera.. are analysed. Weather and lighting conditions (which can contribute to an accident) also need to be included in the assessment, but these conditions can hinder traditional data collection methods.

Terrestrial Laser scanning technology is currently being deployed by police organizations and surveyors for a variety of applications, including accident reconstruction. Since an accident can happen at any time, rain, snow and darkness, traditional data collection methods such as photogrammetry can be limited. TLS devices, that are rated to operate in inclement weather as well as independent of ambient lighting, are ideally suited for quick, accurate and efficient on-site data collection in virtually any circumstance.



Image 2.7 – Point cloud of the scene of an accident

- Land deformation monitoring

This document talks about Land deformation monitoring. Land deformation monitoring is a type of object monitoring. The purpose of Land deformation monitoring is the detection of physical changes in a surface land or target in relation to the environment that surrounds it. To visualize these changes it is necessary to measure different scans of the target after a time and then compare the resulting scans. Land deformation monitoring is a very recent application for TLS technology; this is why there are still many dark points in this field.

CHAPTER 3 : DATA ANALYSIS

After analysing the main functioning and types of TLS devices we will start the Experimental part of this document. The objective of this chapter is to explore the capabilities of TLS instruments for land deformation monitoring applications.

3.1. Available experimental data

To carry out this analysis, we used data obtained from three different environments:

- Castellfolit village
- The experiment at the Campus
- Formigal village

3.1.1. Castellfolit village

The data of the experiment carried out in Castellfolit village was given to the Institute of Geomatics by “The research group of Natural Hazards of the University of Barcelona”. The given data was used to gain experience and study the TLS behaviour on different types of surfaces.

Castellfolit is a village located in the province of Girona. The village, image 3.1, is situated at the top of a cliff. The data obtained from this environment is very useful due to the wide variety of surfaces, colours and shapes present. Since the aim of the experiment is to test the accuracy of the TLS instrument, these characteristics are interesting when comparing the different acquisitions obtained.

The TLS device used to capture the data from this scenario was an Optech ILRIS-3D.

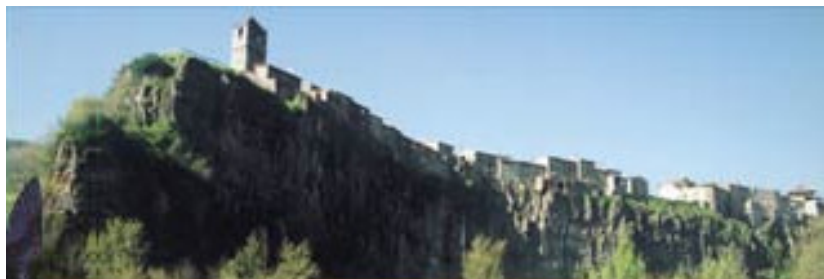


Image 3.1 – Photograph of Castellfolit village

3.1.2. Experiment at the Institute of Geomatics

The objective of this second experiment was to evaluate the capabilities of a developed procedure at the Institute of Geomatics (IG) for land deformation measurement. For this reason we created an emulated testfield at the outside of the IG building.

The testfield consisted of 10 panels, each of which measured 120 cm in height and 60 cm in width. The front surfaces of the panels had different shapes on them and were made of different types of material in order to study the behaviour of the Laser Scanner, depending on the characteristics of each surface. The pannels were positioned securely, to avoid errors caused by environmental conditions, mainly caused by wind. Image 3.2 shows the scenario that was set up to take the measurements:



Image 3.2 – Photograph of Scenario outside the IG building taken by TLS Device

Once all the equipment was ready, acquisitions were taken with two different instruments, a Total Station and a TLS. Measurements with the Total Station are needed to contrast the data obtained from the TLS. The reason for this is that the Total Station is an instrument that has been used in this field for a considerable time and it has been proved that the results are reliable, so they can be used as a reference for results obtained with the TLS device. Once the data was acquired, the movement was emulated by moving the 10 panels from the test field either by traslating or rotating them. Then, measurements were carried out with both devices again.

A Total Station is an optical instrument used in modern surveying. It is a combination of an electronic theodolite¹ (transit), an electronic distance measuring device (EDM) and software. In this case we used a TRIMBLE device.

¹ A **theodolite** is an instrument for measuring both horizontal and vertical angles.



Image 3.3 – TRIMBLE Total Station

This instrument determines the angle and the distance from the instrument to a single point to be surveyed at a time. The EDM sends out an infrared beam which is reflected back to the unit by a prism, situated on top of the point to be calculated, and the unit uses ToF measurement to calculate the distance to the mentioned point. With the aid of trigonometry, the angles and distances are used to calculate the coordinates of the actual position (X, Y, and Z) of surveyed points, or the position of the instrument from known points.

To carry out the measurements of each pannel with the Total Station we created an average of 20 random points along each pannel. These points were measured one by one and then the reference co-ordinate system was calculated.

The second device used for this experiment was a Terrestrial Laser Scanner. The TLS used for the experiment was the Optech ILRIS-3D.



Image 3.4 – Optech ILRIS-3D

In the following table we can find the most important technical overview and specifications for the used device, Optech ILRIS-3D :

Table 3.1. Optech ILRIS specifications

Dynamic scanning range	3 m - 1,500 m
Data sampling rate (actual measurement rate)	2,500 points per second
Beam divergence	0.00974°
Minimum spot step (X and Y axis)	0.00115°
Raw range accuracy	7 mm @ 100 m
Laser wavelength	1,500 nm
Digital camera	Integrated digital camera (CMOS sensor) optional external camera
Scanner field of view (ILRIS-3 ₆ D)	-20° through 90° (V) x 360° (H)
	-90° through 20° (V) x 360° (H)
Scanner field of view (ILRIS-3D)	40° x 40°

The readings with this device were taken from two different positions, 100m and 200m from the test field. The registered data from 100m was taken with a resolution (approximately the distance between each point in the point cloud) of 7mm whereas the resolution for the data registered from 200m was 12mm.

3.1.3. Formigal village

After having set up an emulated scenario to create land deformation, we needed a real case and scenario to verify the obtained results. To obtain this scenario a group of people from the IG travelled to Formigal, in Valle de Tena, Aragón, and took some data acquisitions. This scenario was chosen because there have been important landslides detected lately. In the following image the scenario can be observed:



Image 3.5 – Formigal Scenario photograph

Opposite from the Castellfollit scenario, this is not an ideal scenario for TLS measurements due to the wide areas of grass. Furthermore, the bad weather

and the wind during the measurements, and also the roadworks that were being carried out can affect data quality and therefore, the final results.

Various Scans were taken at two different periods of time, in July and in October 2006.

3.2. Data analysis

After all the data were acquired they were treated and studied in order to finally obtain the required results for the aim of this work, to verify the IG procedure for land deformation measurement on a real landslide case. Below, the main critical points treated during this analysis are described:

- Co-registration of point clouds
- Precision analysis
- Comparison of residuals and photographs.
- Comparison of the incidence angle of the target and the residuals.
- Standard deviation of data.

3.3. Matching

Since laser scanner is a line-of-sight instrument, in many situations the target or scenario has to be scanned from different viewpoints in order to completely reconstruct it. In other cases, several scans from the same viewpoint are made to contrast that the data have been scanned correctly or to verify the precision of the mentioned data. The procedure of joining these different scans together is usually referred to as matching. This procedure involves the matching of point clouds.

In the past, several efforts have been made concerning the surface matching. One of the most common is the ICP, as was explained in section 2.1.1. The proposed method in this document is based on Least Squares 3D surface matching proposed by Gruen and Akca (2005)[7].

3.3.1. Least squares 3D surface matching

The Least Squares Matching (LSM) of digital images was developed in parallel by Gruen, Ackermann and Pertl in 1984. It has been applied to many different types of measurements and feature extraction problems due to its high level of flexibility and its powerful mathematical model.

LSM of overlapping 3D surfaces, matches surfaces that have been digitized/sampled point by point using a Laser scanner device, a photogrammetric method or other surface measurement techniques. In a general view, the used method, Least Squares 3D Surface Matching (LS3D) matches one or more 3D point clouds to a reference 3D point cloud, minimizing

the sum of squares of the Euclidean distances between the point clouds. This method gives the opportunity of matching arbitrarily orientated 3D point clouds.

We assume that two different partial surfaces of the same object are digitized/sampled point by point at different times (temporally) or from different viewpoints (spatially). These two surfaces are discrete 3D representations, one is the template surface $f(x,y,z)$ and the other the search surface $g(x,y,z)$. The aim of this method is to estimate the final location, orientation and shape of the search surface (g), which satisfies the minimum condition of Least Squares Matching with respect to the template surface (f). The following equation represents the functional model:

$$f(x,y,z) - e(x,y,z) = g(x,y,z) \quad (3.1)$$

Where $e(x,y,z)$ are the stochastic discrepancies, which are assumed to be random errors, and may stem from the sensor, environmental conditions or the measurement method. These discrepancies are the difference between the template and the search surface.

The main output is the transformation parameters between the two point clouds which allow to put the two point clouds on the same reference system. This method offers the standar tools of least squares for quality control of the outputs, as for example, the residual which represent the differences between the two point clouds after matching. In this work, the estimated transformation consists on 7 parameters:

- Rotating parameters : $R(\omega, \kappa, \varphi)$
- Translation parameters : $T(x, y, z)$
- Scale factor : m

3.3.2. Matching analysis

To test the matching method we carried out the matching of several scans from the three different scenarios.

First of all, the scans to be matched with the LS3D method from Castellfollit were two scans with overlapping areas taken from different viewpoints. In the following images the overlapping area is indicated by the red square, and only this intersection should be taken into account.

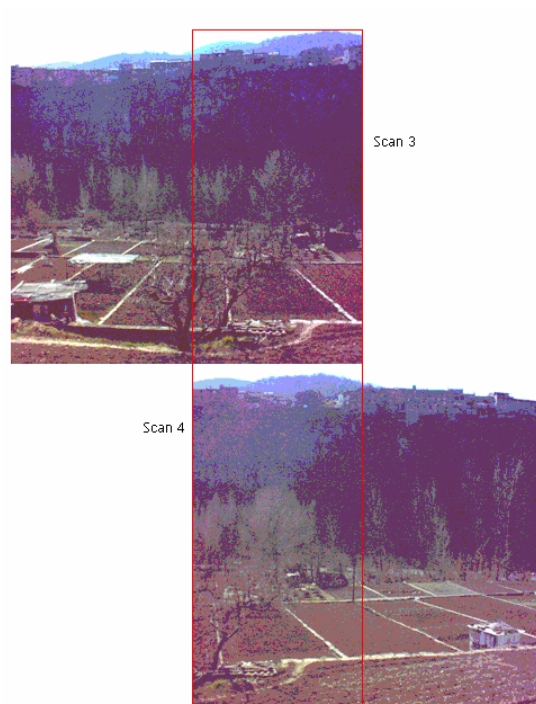


Image 3.6 – Photographs of scans taken in Castellfollit.

In this case, the expected transformation parameters should all be close to 0 except Rotz because the two scans were acquired only rotating the instrument horizontally.

The estimated results and their standard deviation obtained from the registration are shown in the following table:

Table 3.2. Estimated results

Castellfollit 3 - 4		
	Value	Deviation
Scale	1.000000	0.000000
Omega(gon)	0.008	0.00007
Phi(gon)	0.078	0.00026
Kappa(gon)	24.696	0.00007
XO (m)	-0.025	0.00009
YO (m)	0.009	0.00006
ZO (m)	0.002	0.00007
Nºiteracions	6	

The scale factor was fixed because we knew in advance both scans were at the same scale. The estimated results are consistent with the results which were expected to be obtained. The results show that to match both scans, scan 4 has to be moved several centimetres and the Z angle rotated approximately 24 gons (21,6°) to match scan 3.

The residuals obtained from the matching can be seen in the following image:

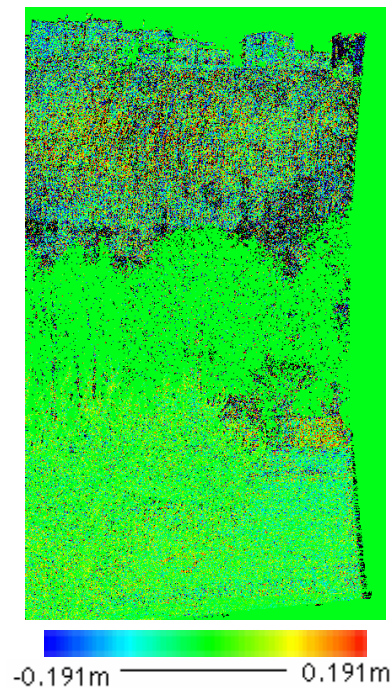


Image 3.7 – Residuals of two matched scans from Castellfolit.

In this case, before matching these point clouds, the main sources of noise were eliminated previously. The residuals are around the order of a millimetre and with a standard deviation in the order of a centimetre which is more or less the expected precision of the instrument. These scans were taken at approximately 400m distance.

The second example of matching analysis was carried out over the Formigal test site, the two matched scans were two scans taken from approximately the same view point, about 550 metres distance, but with a difference of three months in time. In the following images both scans can be visualized:



Image 3.8 – Photograph Formigal taken in July 2006



Image 3.9 – Photograph Formigal taken in October 2006

We can observe that there has been a visible change in these three months, mainly because grass has grown all along the front part. The expected values cannot be previously calculated because of the mentioned differences.

Table 3.3. Estimated results

	Formigal	
	Value	Deviation
Scale	1.000000	0.000000
Omega(gon)	398.585	0.00008
Phi(gon)	1.90	0.00005
Kappa(gon)	399.472	0.00007
XO (m)	-1.960	0.0004
YO (m)	1.945	0.0001
ZO (m)	-0.089	0.0005

The following image shows the residuals, without noise, after matching both Scans from the Formigal scenario:

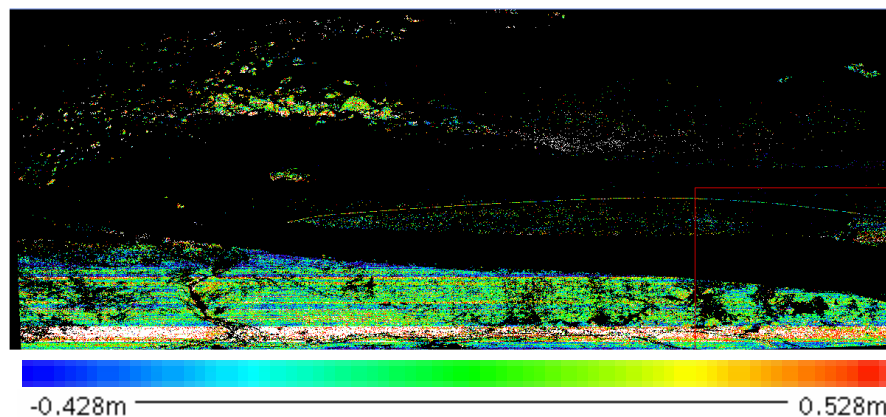


Image 3.10 – Residuals Formigal

The results of this matching are worse than the previous ones, this is mainly due to the characteristics of the area which is not optimal for the angle of incidence viewpoint, for the type of terrain and for the weather conditions during the acquisitions. As was pointed out before, a difference on the land can be seen, turning out to be noise while matching both scans.

Finally, we carried out the exact same test with the IG experiment. In this case, we only used a subsets of the wall with a part of a stair, avoiding this way any possible source of noise,such as vegetation.

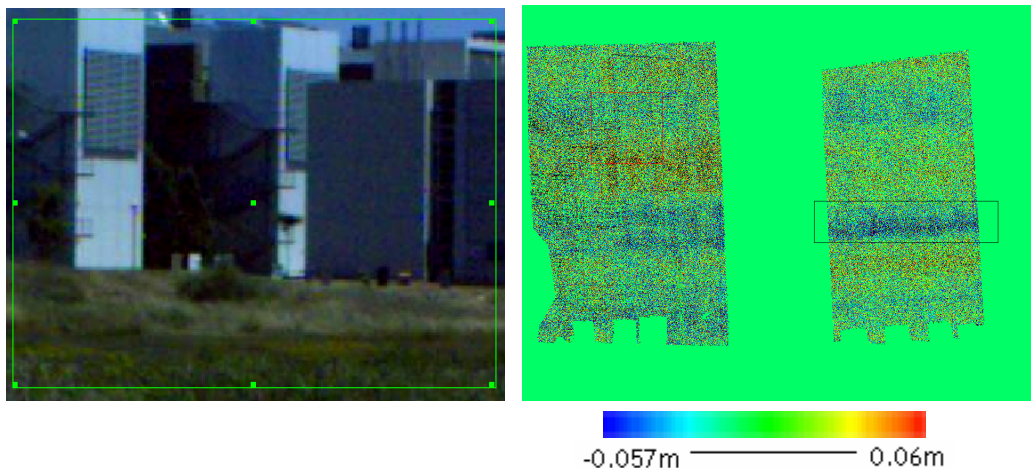


Image 3.11 –Photograph IG Scenario

Image 3.12 – Residuals IG

We can observe the residuals are much better than on the previous scenarios. This is due to the higher resolution and the optimum incidence angle from the surface to the device, in spite of the fact that smooth surfaces are not normally the best kind of surfaces while matching.

Studying the results we detected a strange value on the surface of the wall, marked with a black square. We do not know what it is due to, because the wall is homogenous all along the surface, as can be seen in the photograph. This strange value has probably been caused by sistematic errors due to a bad instrument calibration.

3.3.3. Precision analysis

In this section, one example of precision analysis is presented. Two repeated scans were matched using the LS3D method in order to evaluate the precision of the measurements from the residuals.

The scans to be matched were two scans from Castellfollit which were taken from the exact same position and with a temporal baseline of minutes. Because they were taken from the exact same position there is a total overlap, i.e. the

two scans coincide. The two coinciding images are illustrated in the same image under these lines:



Image 3.13 – Image of Castellfollit Scans

The expected transformation parameters should be close to 0, because of the scans being taken on the same day and from the exact same position.

The estimated results and their standard deviation obtained from the registration are shown in the following table:

Table 3.4. Estimated results

	Castellfollit repeated	
	Valor	Desviació
Scale	1.0000	0.00000
Omega(gon)	0.0068	0.00011
Phi(gon)	-399.9955	0.00015
Kappa(gon)	0.00227	0.00008
XO (m)	0.0062	0.00014
YO (m)	-0.0079	0.00005
ZO (m)	-0.0048	0.00018
Nºiteracions	4	

The residuals obtained from matching both scans have got the appearance illustrated in the following image:

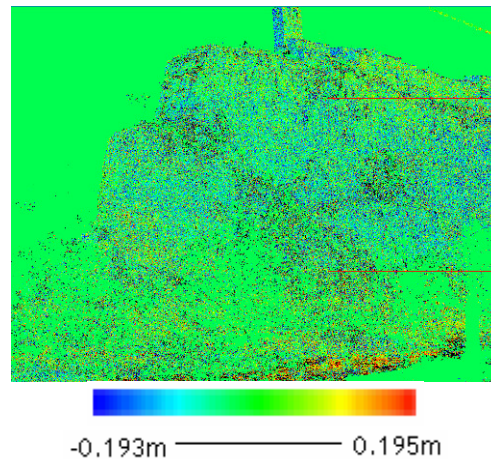


Image 3.14 – Residuals scan 1 and 2

The matching of these two Scans can be used to verify the precision of the data registered from the TLS. The reason for this is that the scans were taken from the exact same position, without moving the TLS, so the results should be really close to 0. As expected, the obtained results are approximately 0 with a difference between both scans in the order of a millimetre and a standard deviation in the order of a centimetre. Although the scans were taken from the exact same position, there can always occur a movement of the vegetation caused by the breeze or the internal instrumentation error of the device. These scans were taken at approximately 400m distance. The precision is consistent with the used device's range accuracy (7 mm at 100 m).

We also carried out several analyses to visualize the behaviour of the residuals over different areas from the scans above:

- Houses
- Rocks with vegetation and without vegetation

The first area to be studied is the tower of the church, as can be seen in the following image:

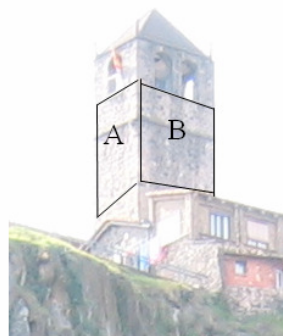


Image 3.15 – Photograph of the tower from Castellfollit

The image shows the characteristics of the target. It consists of a solid tower with two visible walls at different incidence angles, which make the two chosen regions (A,B). The areas with windows and flags were not considered.

For both regions we calculated the statistics which are shown in the following table:

Table 3.5. Statistics for regions A and B

Region	Min (m)	Max (m)	Mean (m)	Stdev (m)
A	-0.04604	0.09108	0.00907	0.01094
B	-0.14362	0.04911	-0.00357	0.01279

The obtained results can be considered as good, they are in the order of a millimetre. Section A and B have got the exact same characteristics, but Section B obtained better results because it has got a smaller incidence angle than section A.

The second area consists of several buildings made of brick with nonparallel walls but with a more or less constant incidence angle and reflectance. In this area several small windows appear. The area can be visualized in image 3.16.



Image 3.16 – Photograph of the group of building.

The statistics of the area are shown in table 3.6.

Table 3.6. Statistics for building region.

Min (m)	Max (m)	Mean (m)	Stdev (m)
-0.13900	0.08300	-0.00390	0.01200

These results are very similar to the obtained for the previous regions, even though this section is further away from the Lidar, so the results should be a little worse. The results are probably as good because in this section we included windows which makes it easier while matching than with smooth surfaces with no structures, like the sections above.

The next sections to be studied are some parts of the rocks which are shown in the following images:

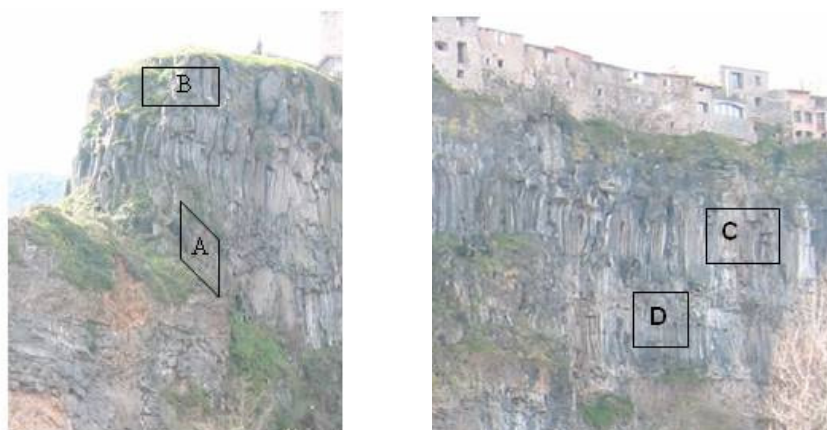


Image 3.17 – Photographs of the rock areas.

On the one hand, A and B are the areas of the rocks closest to the Laser Scanner device. In region A there is a lot of vegetation and it has got quite a big incidence angle, whereas region B has little vegetation and the incidence angle varies within the area. On the other hand, the areas C and D are the furthest away from the Laser Scanner Device. Both areas have no vegetation, area C has quite a constant incidence angle and D has got a big distance variation.

The statistics for the four regions can be seen in the following table:

Table 3.7. Statistics for regions A and B

Region	Min (m)	Max (m)	Mean (m)	Stdev (m)
A	-0.13037	0.1794	0.00175	0.0241
B	-0.16255	0.1717	0.00057	0.01773
C	-0.09023	0.14234	0.00066	0.01683
D	0.044012	0.131496	0.005007	0.014913

To finish, the results for these last sections are better than for the sections of the houses because they have got a smaller incidence angle. We can observe that the rocks with no vegetation, B and C, obtained much better results than the section with vegetation, A. This is consistent, because vegetation always causes noise, resulting in worse results.

3.4. Residuals vs Photograph

The objective of this section is to find out some conclusions comparing the original photograph and the obtained residuals from the registration. We carried out several analyses to visualize the behaviour of the residuals over different areas (houses, rocks, etc.). To carry out the test the matched scans from the sections above were used.

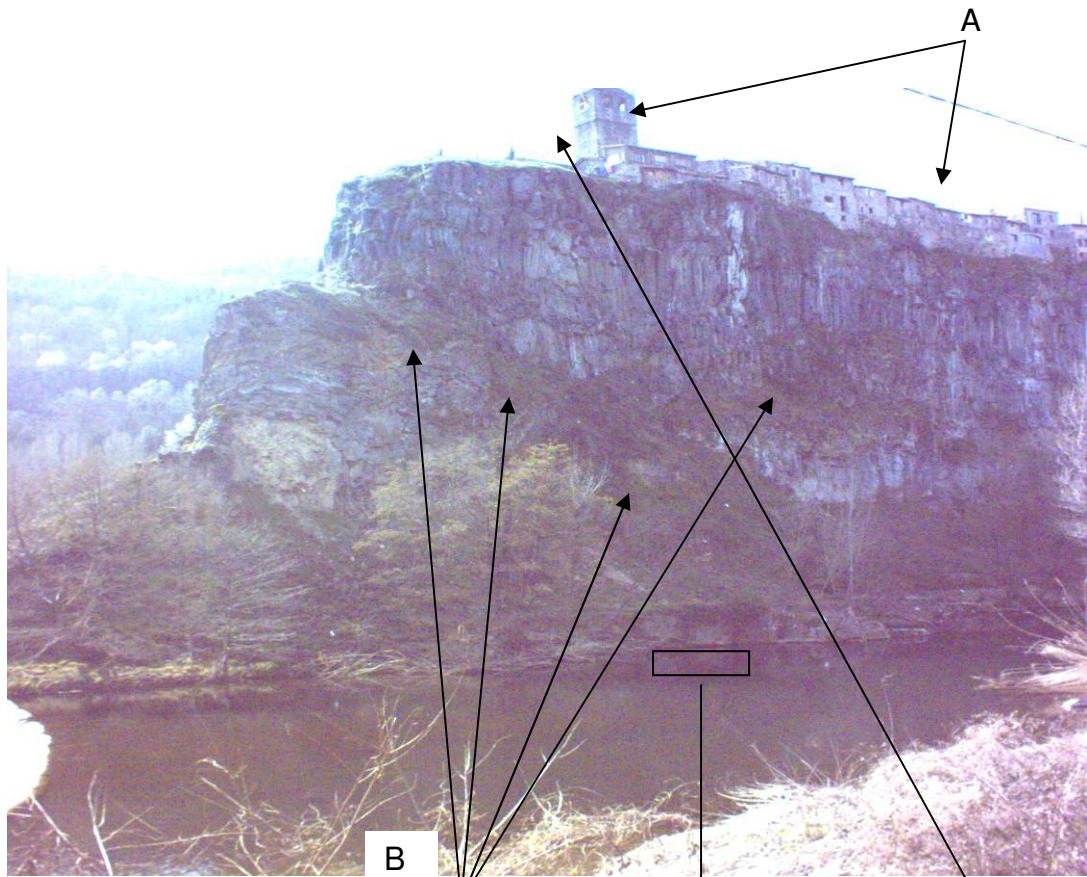


Image 3.18 – Photograph Castellfolit scan

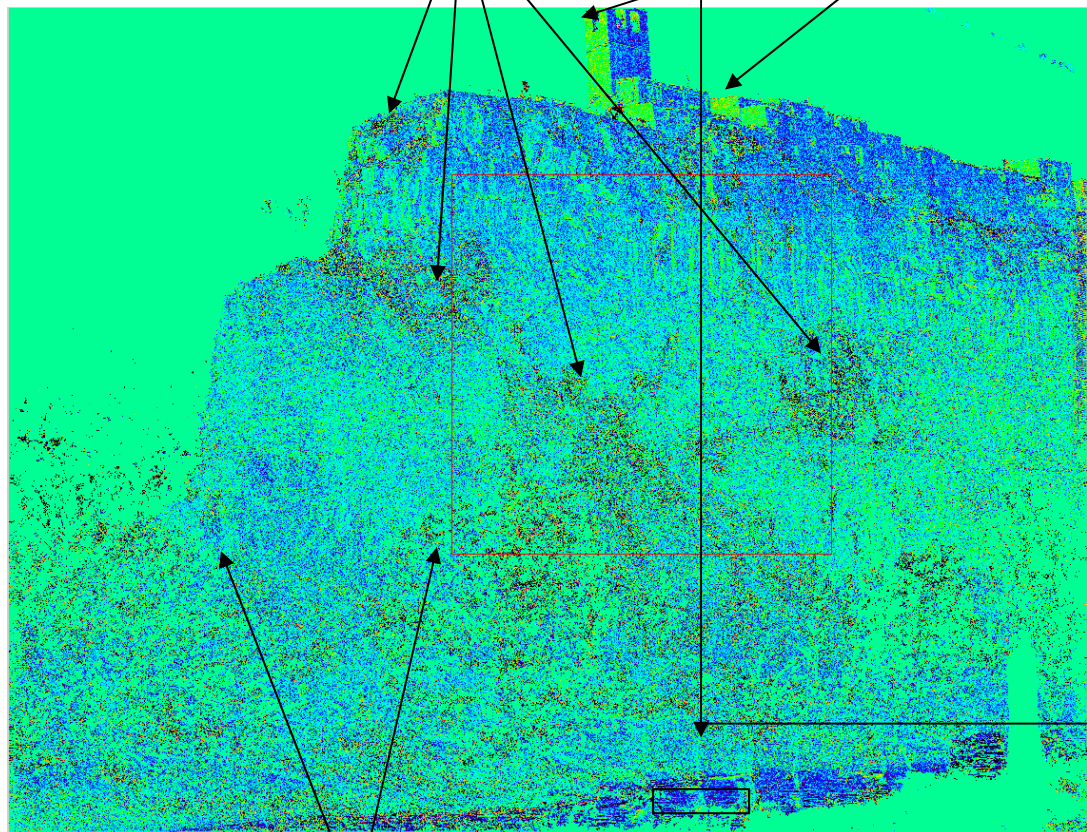
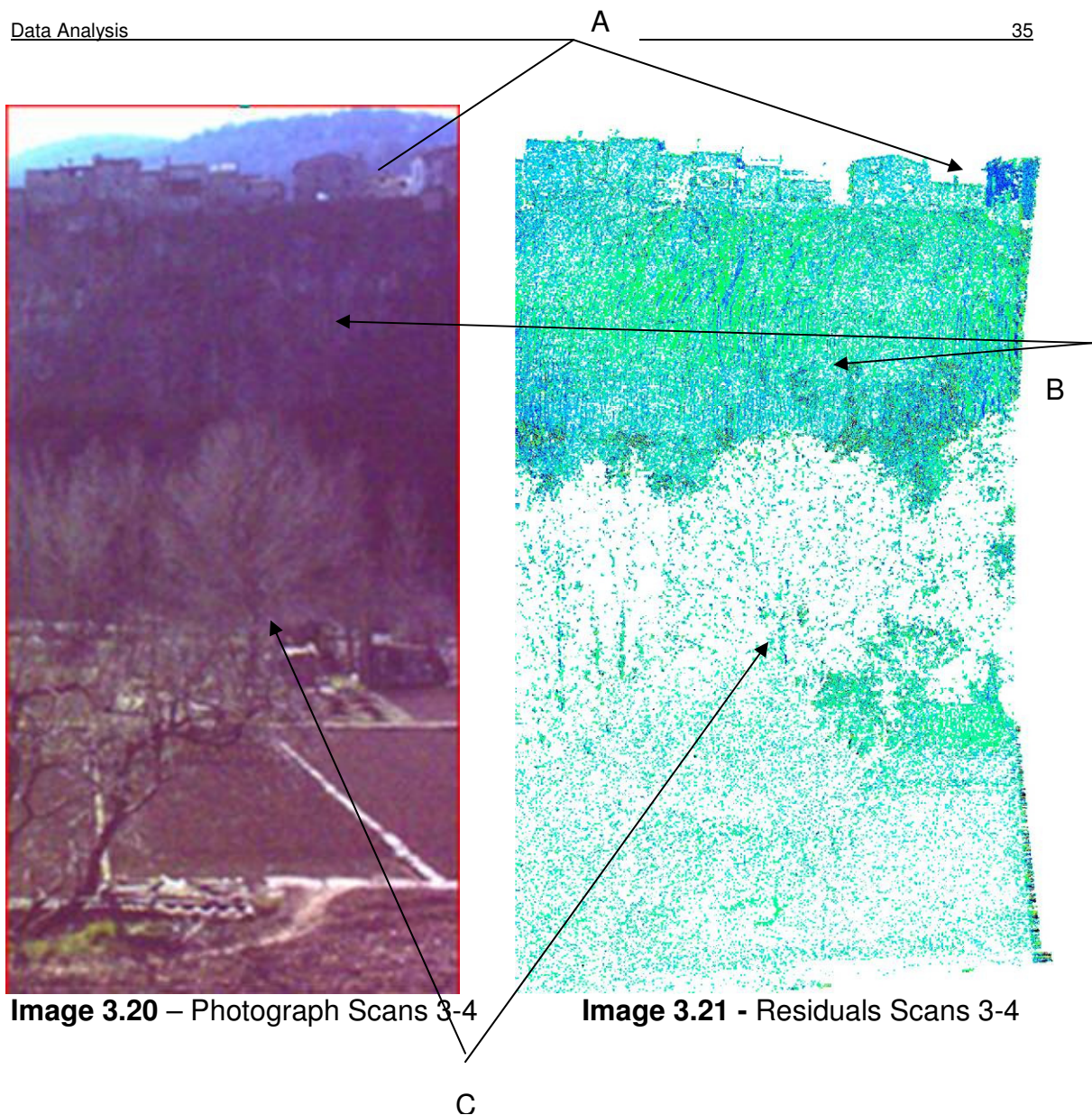


Image 3.19 – Residuals from matching Castellfolit Scans

C



In the images above a comparison between the obtained residual of matching scans and their corresponding photograph can be seen. We have chosen five different areas, which are:

- A: Village area
- B: Areas with vegetation
- C: Areas with trees
- D: Surfaces of the village with same orientation
- E: Area with water

The conclusions obtained from this test are that depending on the type of surface or shape that is being calculated a big difference in the results of the residuals can be found. The part of the field scan where the village is reflected (A) is the surface which obtained the best residuals whereas surfaces composed of trees or vegetation (B) gave the worst residuals. The reason for this is that the houses are made of a solid non-variable surface, surface which is not affected by external conditions such as wind, so it is logical that when matching, the readings coincide almost exactly. In contrast, when dealing with surfaces with a degree of movement, like vegetation, it is very difficult for the

TLS to get the same reading twice. In conclusion, readings of trees and vegetation result in noise, so previous to matching these areas should be discarded.

In the scans, a strong correlation can be visualized on the surfaces marked D. This correlation, which is studied in the following section, could be due to the orientation of the targets with respect to the TLS.

Finally, E seems to be the reflexion of the rocks in the water, as if the beam had landed on the water and the reflexed beam had bounced off the rocks and returned to the TLS.

3.5. Incidence angle vs Residual

The goal of this test is to study the relation between the incidence angle of the targets and the precision by using the residuals. To find out this relation, we calculate the incidence angle for every point in the point cloud and use the residuals obtained when matching the images from the TLS in the LS3D matching method explained before.

The incidence angle is calculated for every point in the resulting point cloud from the TLS instrument. The procedure used to calculate the incidence angle is documented below and the used programme can be seen in Annex [1] .

The reference of the coordinate system is the TLS geometric rotation centre, which is considered as the zero point (0,0,0). To calculate the angle of incidence we need two vectors, as is shown in image 3.22:

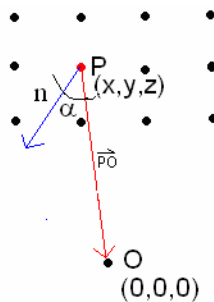


Image 3.22 – Needed vectors to calculate the incidence angle of point P.

Where P is the point to calculate, O the center of the TLS and n the normal vector.

The PO vector is calculated directly from two known points, the zero point and P.

$$PO = P - O = (X,Y,Z) - (0,0,0) = (X-0,Y-0,Z-0) = (X,Y,Z) \quad (3.2)$$

The normal vector (n), on the other hand, is calculated by multiplying two vectors that are created from the nearest existing points to the respective point in the point cloud. The result of the vectorial product between the two vectors represents the normal vector to the surface. In image 3.18 we can visualize the two vectors and the resulting normal vector:

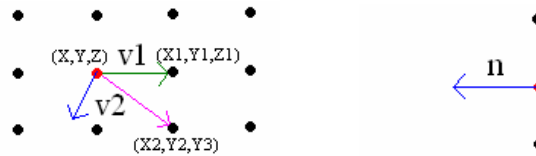


Image 3.23

The mathematical procedure to calculate the normal vector is to calculate the vectorial product between the two vectors:

$$\begin{aligned} V1 &= (X,Y,Z) - (X1,Y1,Z1) = (v11,v12,v13) \\ V2 &= (X,Y,Z) - (X2,Y2,Z2) = (v21,v22,v23) \end{aligned} \quad (3.3)$$

$$N = V1 \times V2 = \begin{vmatrix} i & j & k \\ v11 & v12 & v13 \\ v21 & v22 & v23 \end{vmatrix} = (v12 \cdot v23 - v13 \cdot v22, v11 \cdot v23 - v13 \cdot v21, v11 \cdot v22 - v12 \cdot v21) \quad (3.4)$$

Lastly, after calculating the Normal Vector and the PO vector we obtain the incidence angle by calculating the scalar product of the two mentioned vectors with the following formula:

$$\cos \alpha = \frac{V1 \cdot V2}{|V1| \cdot |V2|} \quad (3.5)$$

As for most of the other tests we carried it out with two different scenarios to contrast results. The first scenario was Castellfollit and the following images are going to be compared:

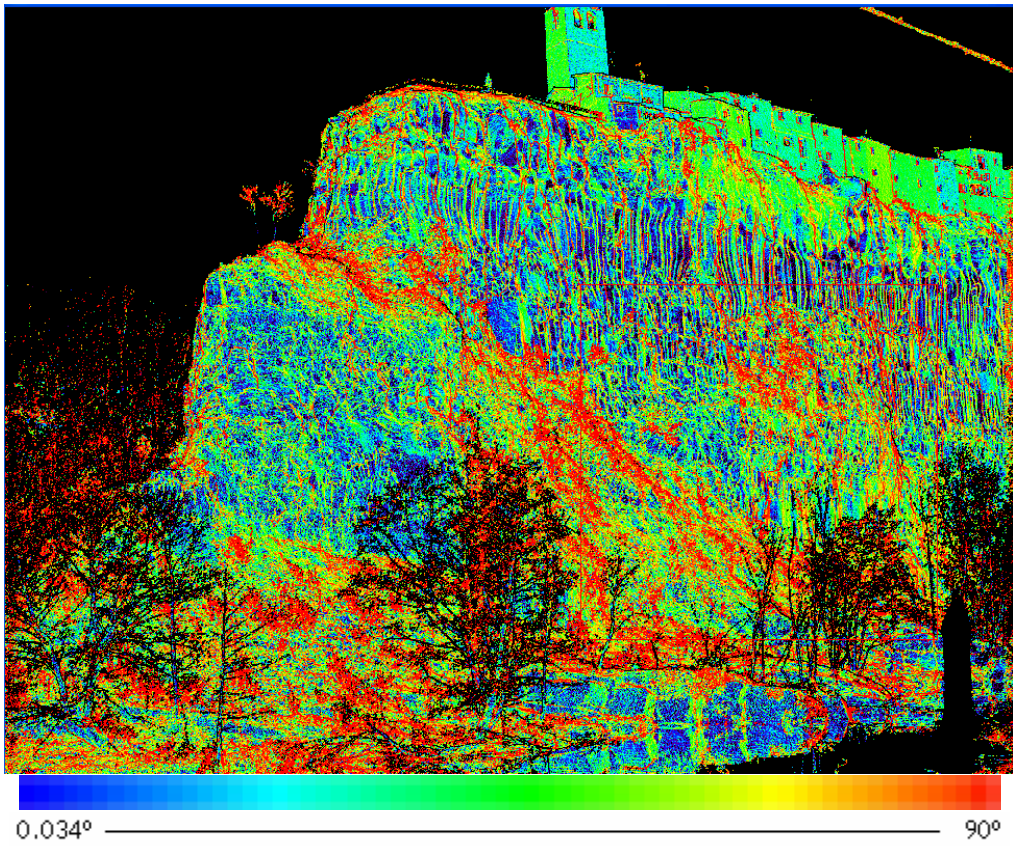


Image 3.24 – Incidence Angle Castellfollit

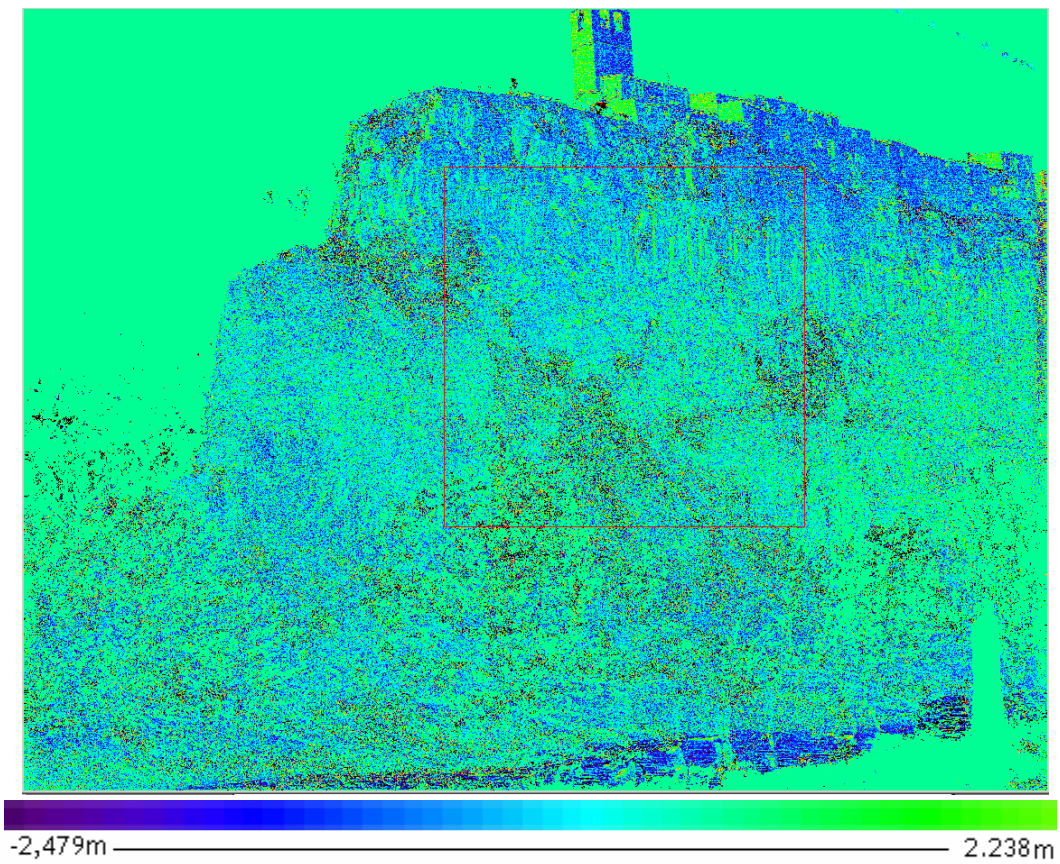


Image 3.25 – Residuals Castellfollit

Firstly, we calculated the statistics for different incidence angle intervals. We grouped the incidence angles in intervals of 10, then we calculated the statistics of the residuals of the points with the mentioned incidence angle values. The obtained results were the following:

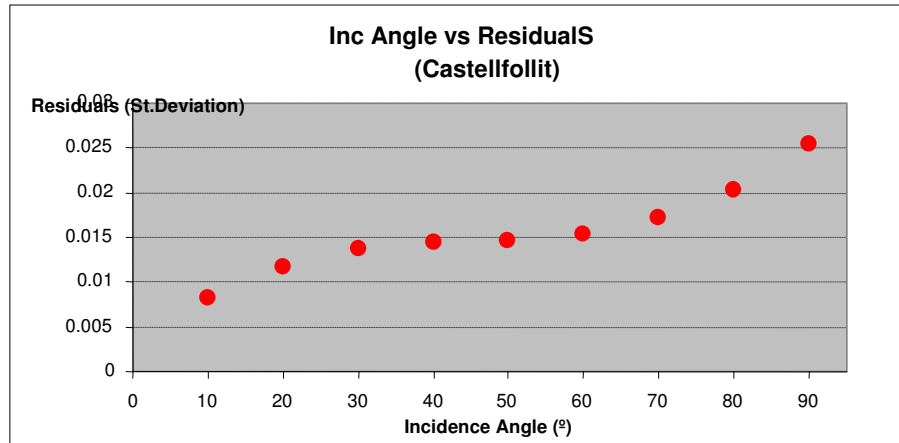


Image 3.26 – Inc Angle vs Residuals for Castellfollit Scans. X corresponds to incidence angle intervals. Y corresponds to the St.Deviation of the Residuals.

The following scans correspond to the residuals and the incidence angle of two parts of the wall, as is shown:

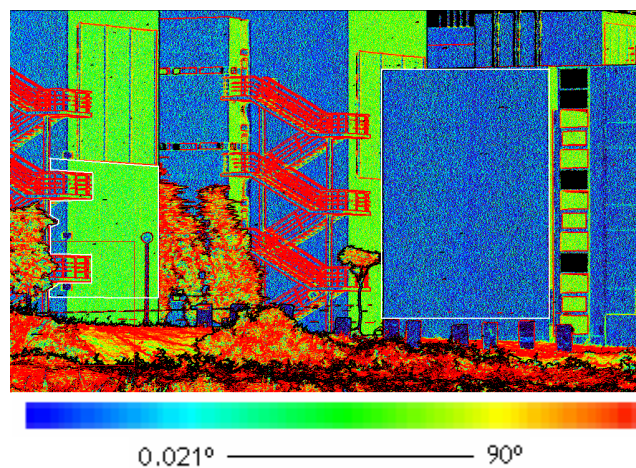


Image 3.27 – Incidence Angle – IG Scenario

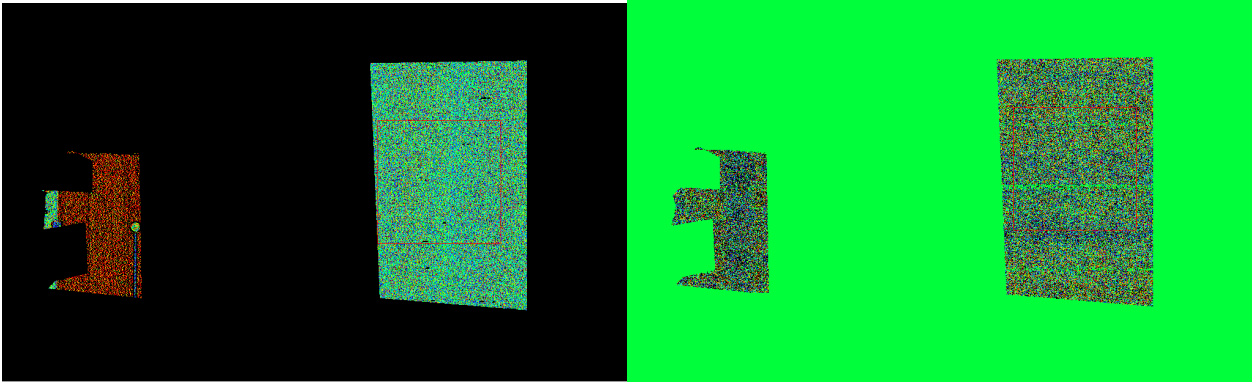


Image 3.28 –Incidence Angle IG Institute

Image 3.29 – Residuals IG Institute

The same procedure as before has been carried out for this scenario:

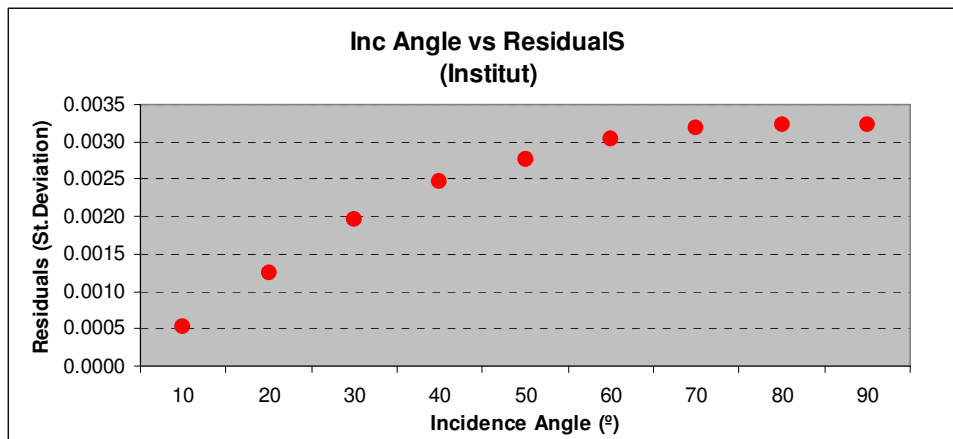


Image 3.30 – Inc Angle vs Residuals for IG Institute. X corresponds to incidence angle intervals. Y corresponds to the St.Deviation of the Residuals.

The obtained results from both scans conclude that the bigger the angle of incidence, the higher the Residuals value. This means that there is a higher dispersion of the data as the angle of incidence increases. This can be explained because the bigger the incidence angle, the less energy the TLS receives from the target, so the higher the possibility of error.

3.6. Analysis of Standard Deviation measurements

In this section we calculate the Standard deviation to find out or differentiate the parts of the scan that are rougher. The Standard Deviation of values is a measure of the spread of its values. In this case we calculate the Standard Deviation of a point in reference to the points in a chosen window, the bigger the standard deviation value, the rougher the surface of the calculated target. We do this to try and find out the possibility of using the standard deviation to locate the similar parts in two different scans. To do it we calculate the standard

deviation of the distance for every point in the point cloud using a chosen window, as can be seen in the following image:

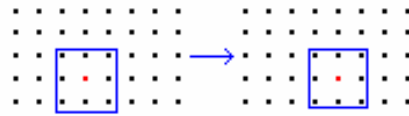


Image 3.31 – 3x3 Window to calculate the Standar deviation of the red point.

The window consists of all the points round the point to be calculated. The used programme can be seen in Annex [2].

To continue with the same criteria as in the other tests, this test will also be carried out with two different scenarios. The first chosen scenario is Castellfollit.

In the following images, the Standard Deviation and the Incidence angle of the entire used scan, can be visualized. We have used a subset where there are no trees, because trees cause noise and make the calculated data not as precise.

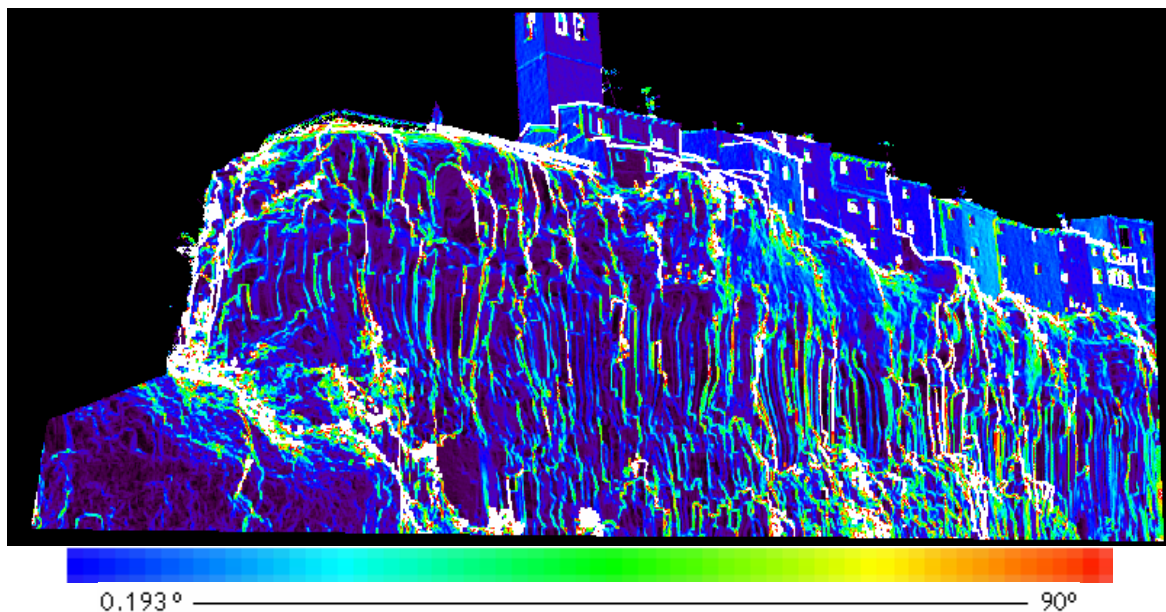


Image 3.32 -Incidence Angle Castellfollit subset

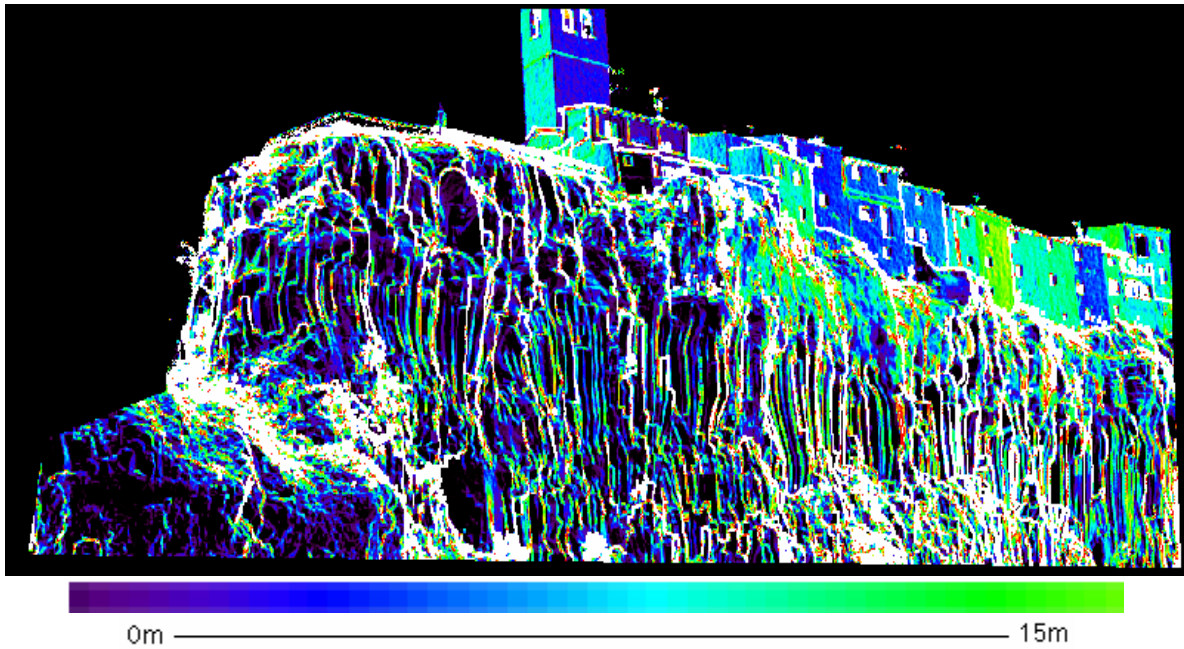


Image 3.33 - Standard Deviation Castellfolliit Subset

To make a comparison between the Standard Deviation and the Incidence angle we made up a graphic for different Standard Deviation ranges. We grouped the Standard Deviation in intervals of 0.01, then we calculated the statistics of the incidence angle of the points with the mentioned Standard Deviation values:

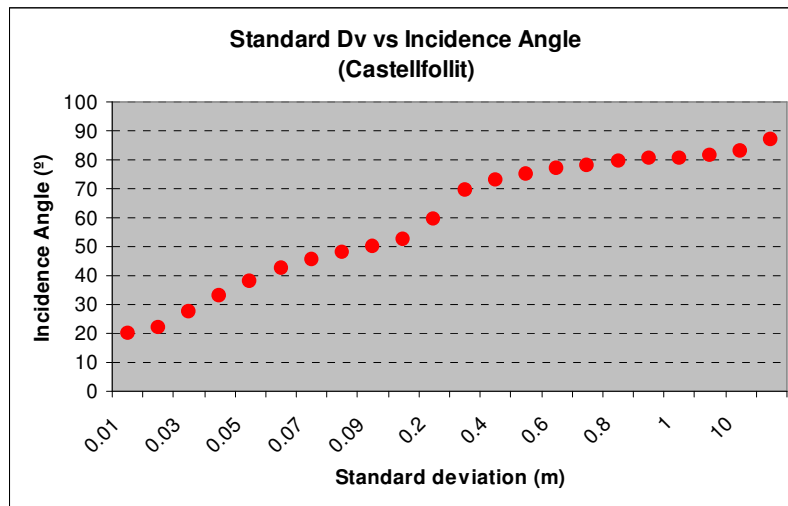


Image 3.34 – Standard Deviation and Incidence angle Castellfolliit. X corresponds to Standard Deviation intervals. Y corresponds to the Incidence Angle.

The following two scans to be compared correspond to a subset from Formigal. In this case we have chosen a subset where a group of rocks are located:

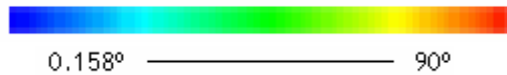
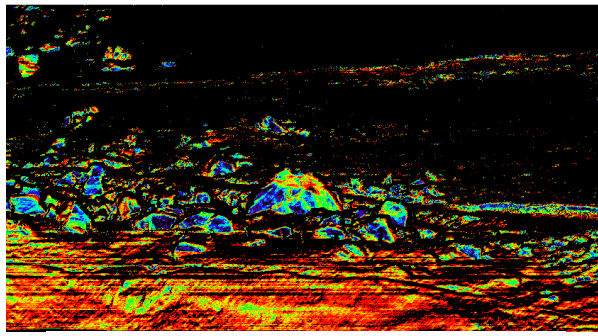


Image 3.35 - Incidence Angle

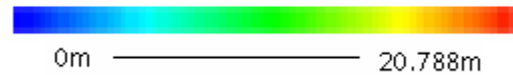
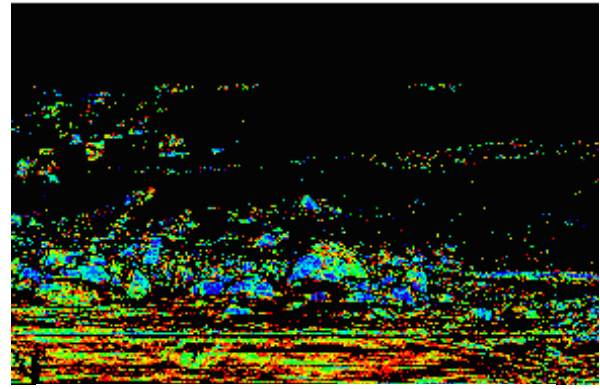


Image 3.36 - Standard Deviation

In this case, to make the comparison between the Standard Deviation and the Incidence angle we made a graphic for different Incidence Angle ranges. We grouped the Incidence Angle in intervals of 10, then we calculated the statistics of the Standard Deviation of the points with the mentioned incidence Angle:

:

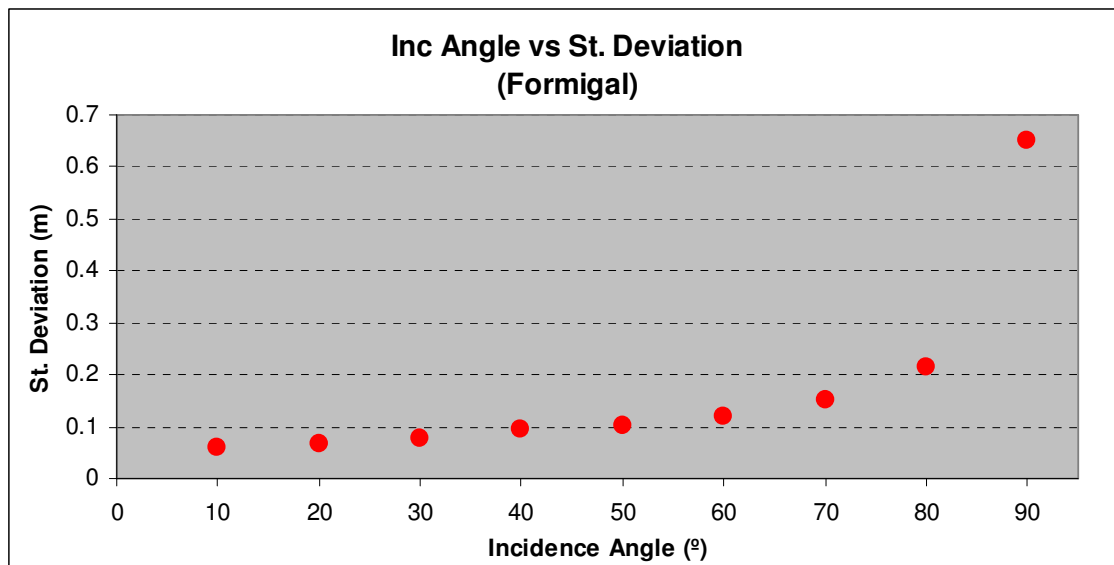


Image 3.37 – Inc Angle vs Standard deviation. X corresponds to Incidence Angle intervals. Y corresponds to the Standard Deviation.

In both cases we can observe that the bigger the angle of incidence, the higher the Standard deviation of the calculated data from the TLS. The same reason as for the above case causes this, the bigger the incidence angle, the less energy the TLS receives from the target, so the higher the possibility of error. We can visualize that on the outlines of the objects standard deviations are very high compared to the rest of the object.

3.6.1. Use of Standard Deviation value

In this section we will try and find out the possibility of using the Standard deviation to locate same areas in two different scans taken at a different baseline of time or from a different point of view. We think that if the scans are taken at different baselines of time but more or less from the same position, we will probably be able to detect and locate the different areas from the Standard deviation. Whereas we are not as sure that it will be possible if the scans are taken from different view points, due to the possibility of the targets changing the shape, so the Standard deviation can also change. If it is possible to locate this areas, they will be very useful as initial values for co-registration.

First we will study this with the data obtained from Formigal, because we have got two scans taken at different periods of time, one in July and the other in October. In the following image, both scans can be visualized:

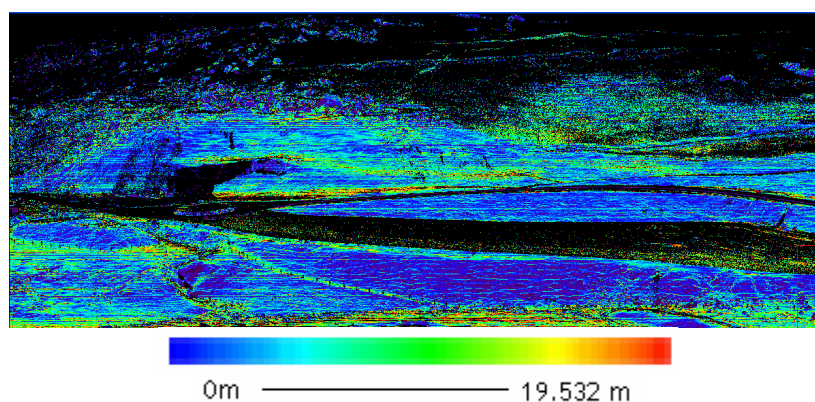


Image 3.38 – Standard Deviation Formigal in July 2006

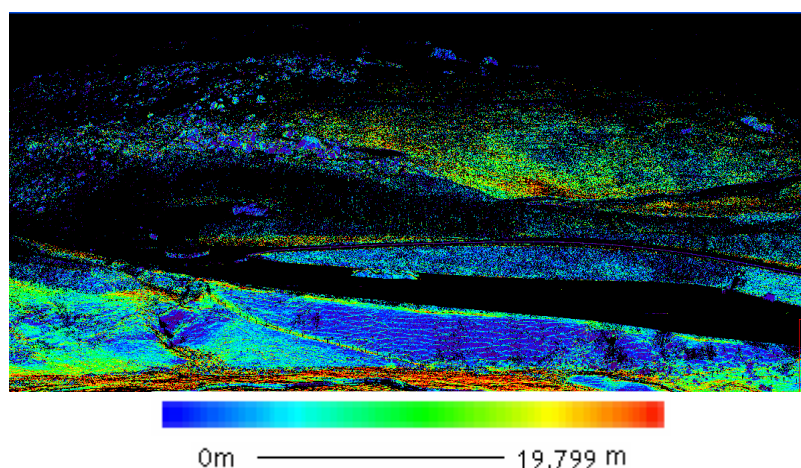


Image 3.39 - Standard Deviation Formigal in October 2006

As can be observed, both images were taken from a very similar point of view but with three months difference. This is a short period of time, but as was

mentioned in previous sections, there was a big change on the area. We have chosen two different subsets of data which we think could make it possible to locate different targets in the scans.

The first subset corresponds to the lowest standard deviation values, from 0 to 5 cms. Here we show the resulting images of both scans:

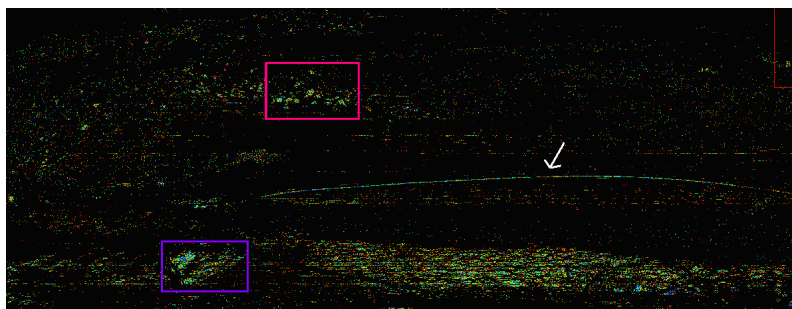


Image 3.40 – 0-5cms Standard Deviation in July 2006

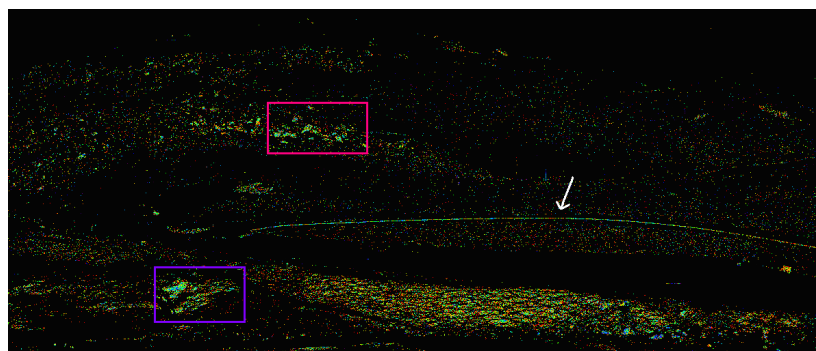


Image 3.41 – 0-5cms Standard Deviation in October 2006

In the images the similar located targets in both scans have been marked. They correspond to some rocks, a place where there was like a hole and the fence from the road. With these located targets it could be possible to find several points as reference points or areas to start with the matching.

The second subset corresponds to the highest standard deviation values. This values can gives us both, the outlines or noise data or some other reference targets. In the following images the scans can be visualized:

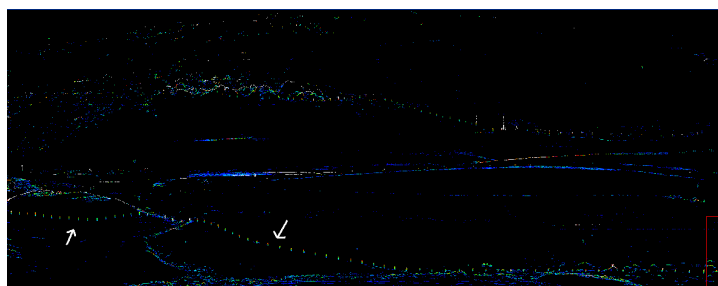


Image 42– max Standard Deviation Formigal in July 2006



Image 3.43 – max Standard Deviation Formigal in October 2006

We can visualize in both scans all the poles from a fence. In this case there are no wrong points because there are no trees or bushes that would result as noise. This is why we will carry out this last experiment with Castellfollit, which has got a lot of trees and vegetation:

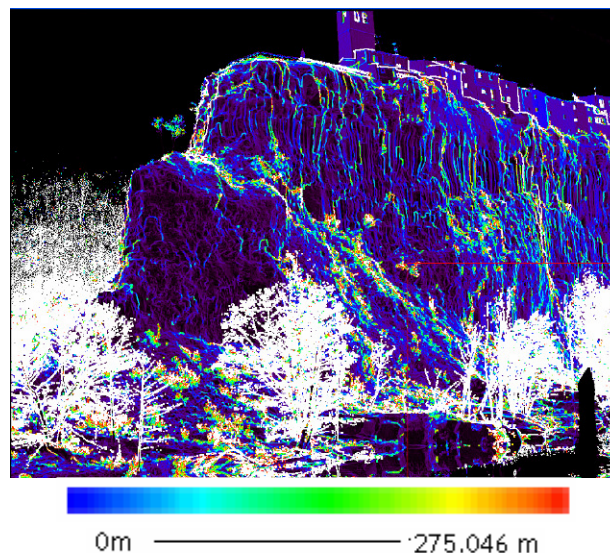


Image 3.44 - Castellfollit Scan1

In image 3.44, we can observe that there are very high values that correspond to bad points. These bad points will be due to noise. To eliminate this noise, we will look for a high range of Standard deviation, because these bad points should have quite a different value compared to the right ones. In the following image the values correspond to the ones from 1m to the maximum (275m):

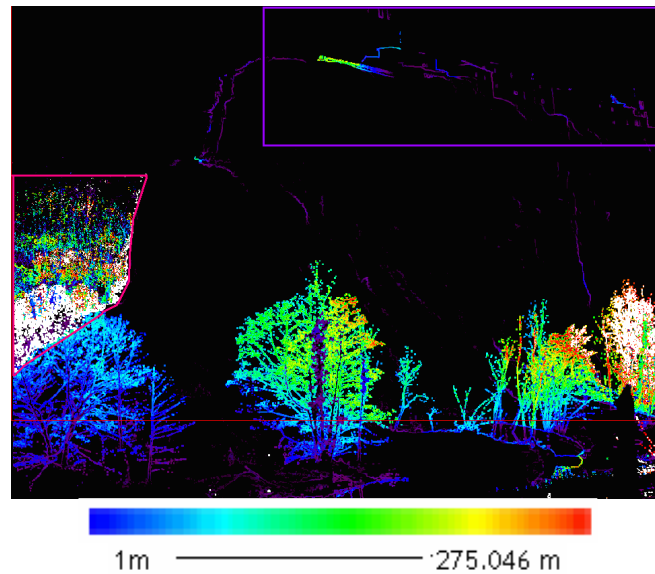


Image 3.45 - Noise in Castellfollit

We have been able to eliminate most of the bad points by simply eliminating the highest values of Standard Deviation. In this case it is possible to do this because there is not a very big distance between the targets in the image. In the purple square there are some good points, the outline and windows of the houses that shouldn't have been eliminated..To solve this we just need to select the area and not apply the mask. The data in the red square has been eliminated directly, because looking at the digital photograph we can observe it corresponds to the forest behind the mountain, so it is data that will only provoke bad results

In the following image we can visualize the resulting scan without vegetation:

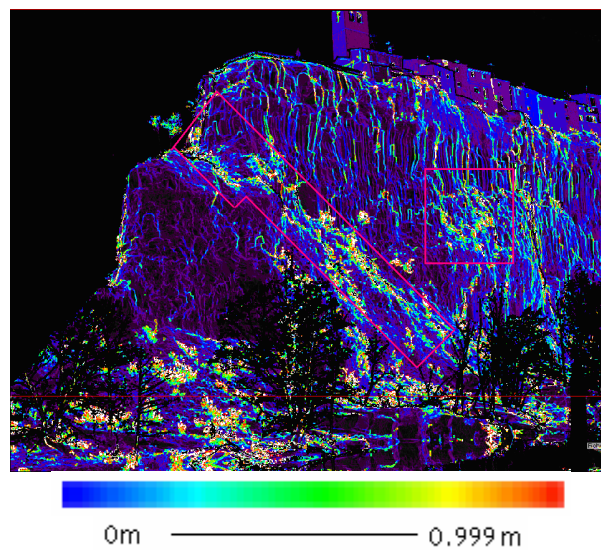


Image 3.46 – Castellfollit Scan without noise

We can observe in the image, that the smallest vegetation, like little bushes in between the rocks haven't been eliminated. In some occasions, it would be better to eliminate this data, but because it is part of the rocks and the scenario it is not necessary.

After using scans taken from the same view point, we will try and locate similar parts in two scans taken from different view points. The scans we are going to use for this section are the following:



Image 3.47 - Scan4

Image 3.48 - Scan5

In the following images the scans can be visualized after applying the Standard Deviation:

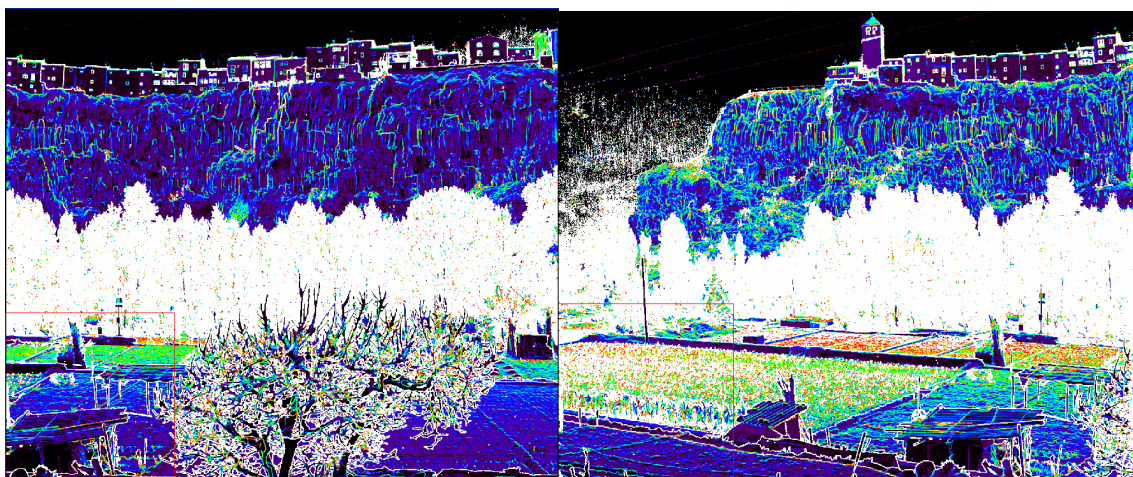


Image 3.49 – Standard Deviation

Image 3.50 – Standard Deviation

In this case we will create a mask that will include the range from 0 to 2 m. Here we show the resulting images of both scans:

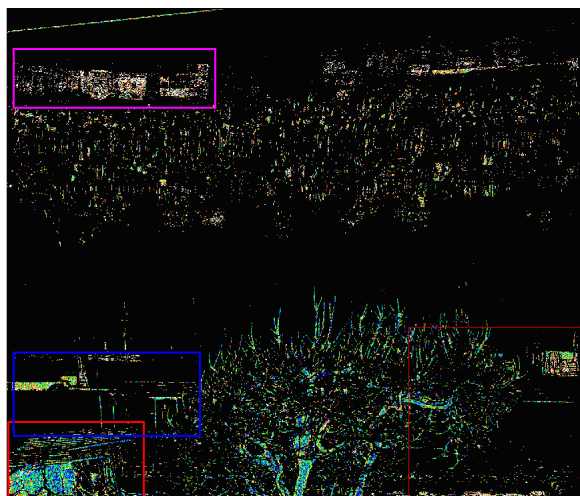


Image 3.51 - Scan4

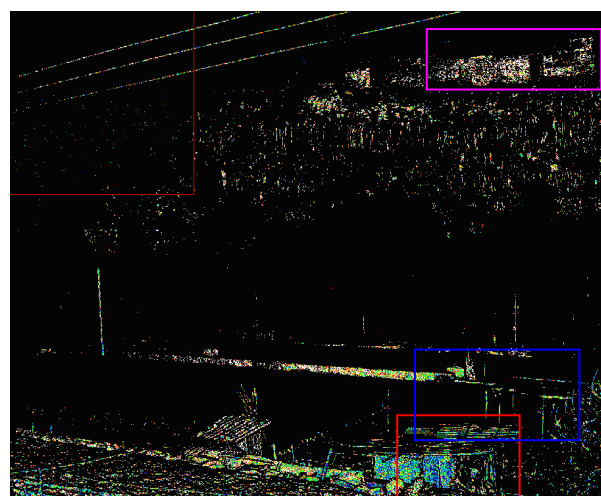


Image 3.52 - Scan5

The similar targets in both scans have been marked with different squares. In this case they correspond to some houses in the village and a little cottage in the fields. These points could be used as reference points to start the matching.

In conclusion, the standard deviation can be used to find initial reference points for both cases, scans taken from different viewpoints, and scans taken from the same viewpoint but a different baseline in time. It can also be used quite effectively to eliminate noise caused by trees or vegetation. To conclude, this is not a good method to be able to distinguish objects automatically, because manual interaction has to be carried out.

3.7. Study of the Influence of the characteristics of the object

As mentioned before, the goal of this test is to study the quality of the measurement realized with the TLS. To study this quality, we will also focus on the dispersion of the point clouds depending on the properties of the material. For this test we will use some subsets from the obtained data in the experiment at the institute. In the following image a photograph of the ten artificial used panels can be seen:

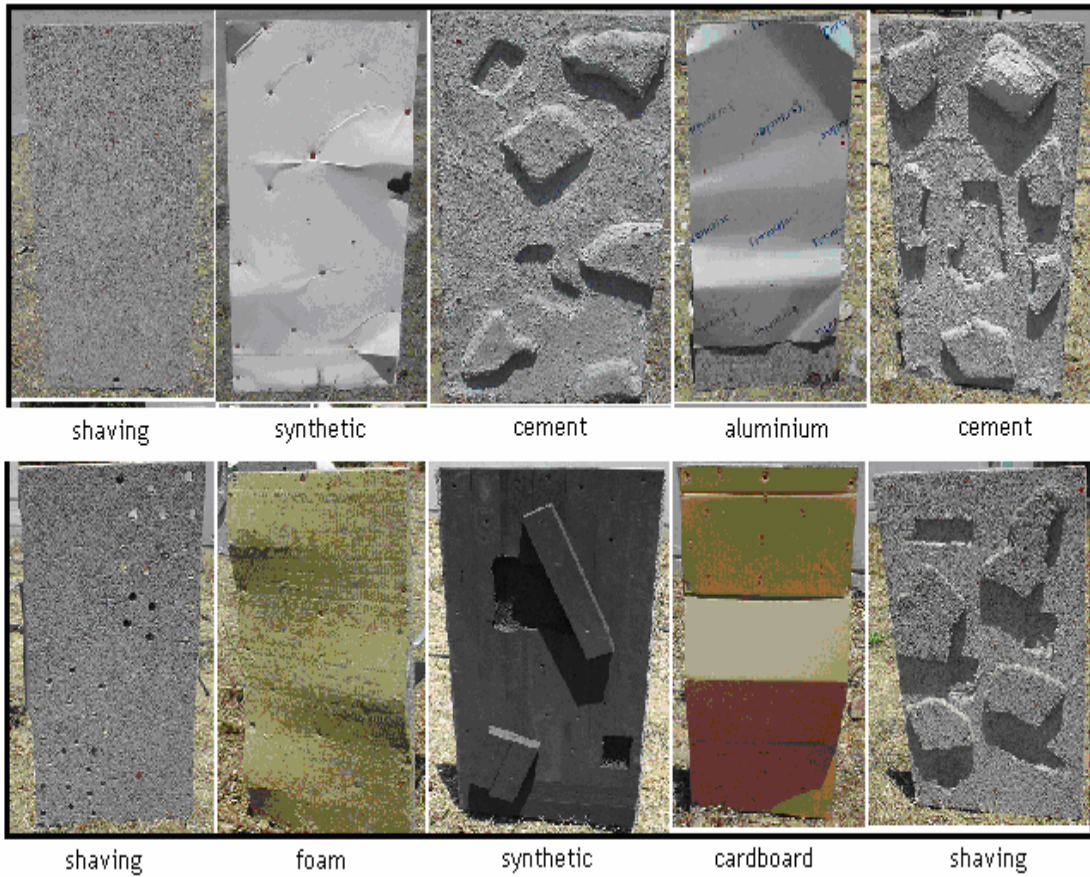


Image 3.53 – Different Panel surfaces from the IG experiment

The number of panel in the image goes from top left starting in 1.

First of all we will verify that the standard deviation corresponds with the shape of the panel, not taking into account the material in this case, just the shape. The theory tells us that the rougher the surface, the higher the standard deviation should be. Here we can find a graph comparing the Standard deviation for the ten panels:

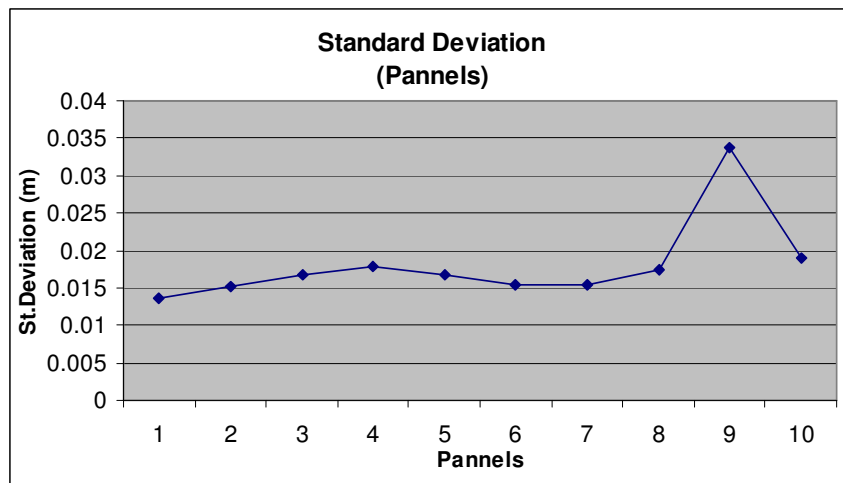


Image 3.54 – Standard Deviation of the distance measured by the TLS Panels

In the graph we can observe that Panel 9 has got the highest standard deviation, this is consistent because it has got the roughest surface, so the difference of values between the points in the point cloud are higher. Whereas for panel number 1 we obtain the lowest value, due to the smooth surface. For the other panels the values are very close because they have all got similar shapes.

Now we will go on to study the effect of the different materials of the panels in the TLS measurements. To do this we will use subsets of the different panels where the surface is smooth, not selecting the different created shapes. An example is shown with panel 3, the parts marked in red are the ones that have been chosen:



Image 3.55 – Smooth subsets chosen for panel 3.

We need to do it this way because to compare different materials it is necessary to have a more or less similar surface (shape) for all the panels. In the following graph the results can be observed:

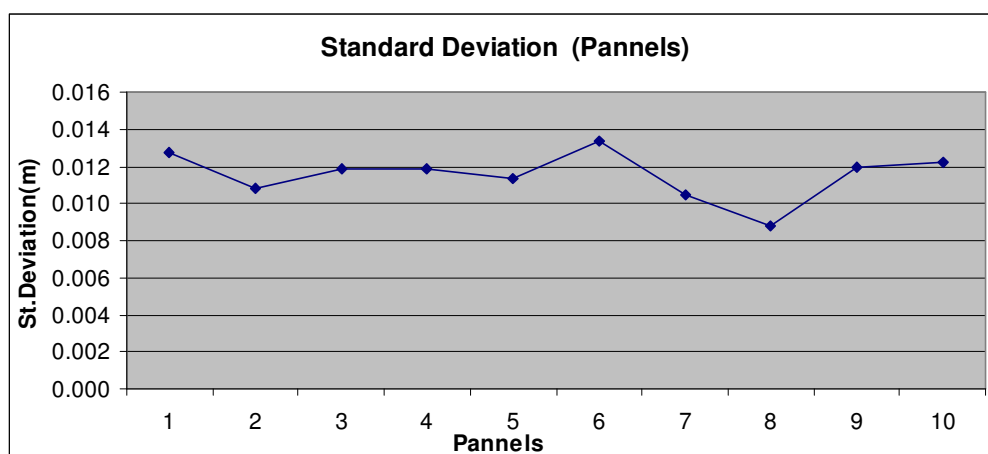


Image 3.56 – Standard Deviation of the distance measured by the TLS of smooth subsets of Pannels

We can see that there are hardly any differences between the different Standard Deviation of the ten pannels, the differences are of a few millimeters. However, the three pannels with the shaving material are the ones with highest values. This is due to the rough and irregular surface, then, it is normal to obtain these values. Opposite, we can visualize that pannel 8 has got the lowest value, this is because it corresponds to the smoothest surface, so the standard deviation is the lowest.

CONCLUSIONS

This project describes the main working principles and functioning of TLS technology and devices. The document also experiments and studies the capabilities of TLS technology in the use of Land Deformation Monitoring. To test these capabilities we carried out several tests in three different scenarios, as was explained in chapter 3.

First of all, TLS could be a good technology for Land Deformation Monitoring because it uses high speed data capture and is an active non-contact range-finding device, which makes the devices capable of working in most real world environments and under a variety of extreme conditions. After knowing this, we tested the accuracy of the obtained data in several scenarios.

The tests gave us some limitations and conclusions while preparing the scenario and while processing the obtained data from TLS devices:

- The type of surface or shape of the monitored scenario affects the obtained results while co-registration. The best results were obtained from solid, rough and non-variable surfaces (buildings), surfaces which are not affected by external conditions such as wind, whereas variable surfaces such as vegetation and trees gave the worst results, so they should be eliminated before co-registration.
- We also concluded that rough surfaces are more optimum for co-registration than smooth surfaces. This is because the more different structures, the easier to match each point with its corresponding point. For smooth surfaces, with no structures, the possibility of error is higher, because of the heterogeneous surface.
- The orientation of the TLS devices to the targets is also an important issue while preparing to scan a scenario. The bigger the angle of incidence, the worse the results, there is a higher dispersion of the data. Therefore we must try and orientate the TLS device perpendicularly to the surface of the scanned targets.
- We found out that the Standard Deviation, dispersion of the data obtained from the co-registration of two scans can be used to eliminate surfaces that cause bad data, such as trees and vegetation. This Standard Deviation can also be used to search for initial reference points to start the matching between different scans.

BIBLIOGRAPHY

- [1] Thorsten SCHULZ and Hilmar INGENSAND, "Terrestrial Laser Scanning – Investigations and Applications for High Precision Scanning", *FIG Working Week 2004*, Athens, Greece, May 22-27, 2004
- [2] Rudolf STAIGER, Germany, "Terrestrial Laser Scanning Technology, Systems and Applications", *2nd FIG Regional Conference Marrakech*, Morocco, December 2-5, 2003
- [3] K.-H. Thiel a, *, A. Wehr, "PERFORMANCE CAPABILITIES OF LASER SCANNERS - AN OVERVIEW AND MEASUREMENT PRINCIPLE ANALYSIS", *Internacional Archives of Photogrammetry, Remote Sensing and Spatial information Sciences*, Vol XXXVI – 87W2
- [4] Paul Bryan Metric Survey Team Leader and Head of the Photogrammetric Unit, Cork, "3D Laser Scanning New techniques of observation", *Conservation bulletin* Issue 45, Spring 2004.
- [5] KERSTEN, T., STERNBERG, H., MECHELKE, K., 2005, "Investigations into the accuracy behaviour of the terrestrial laser scanning system Mensi GS100", 7th Conference on Optical 3D Measurement Techniques, 3-5 October 2005, Vienna (Austria)
- [6] Thomas SCHÄFER and Thomas WEBER, Germany, Peter KYRINOVIČ and Miriam ZÁMEČNIKOVÁ, Slovakia, "Deformation Measurement Using Terrestrial Laser Scanning at the Hydropower Station of Gabčíkovo", *INGEO 2004* and FIG Regional Central and Eastern European Conference on Engineering Surveying Bratislava, Slovakia, November 11-13, 2004
- [7] Armin Gruen, Prof. Dr., and Devrim Akca, Research Assistant Chair of Photogrammetry and Remote Sensing, Swiss Federal Institute of Technology (ETH) Zurich, "LEAST SQUARES 3D SURFACE MATCHING", *ASPRS 2005 Annual Conference "Geospatial Goes Global: From Your Neighborhood to the Whole Planet"* March 7-11, 2005 □ Baltimore, Maryland
- [8] G. Bitelli, M. Dubbini, A. Zanutta, "TERRESTRIAL LASER SCANNING AND DIGITAL PHOTOGRAMMETRY TECHNIQUES TO MONITOR LANDSLIDE BODIES", *Commission V, WG V/2*.
- [9] Derek D. LICHTI and Stuart J. GORDON, Australia, "Error Propagation in Directly Georeferenced Terrestrial Laser Scanner Point Clouds for Cultural Heritage Recording", *FIG Working Week 2004* Athens, Greece, May 22-27, 2004
- [10] NORBERT PFEIFER, 2004, "Development Applications and challenges Terrestrial Laser Scanning", *GIM International* December 2004.
- [11] SCHULZ T., INGENSAND H., "Influencing variables precision and accuracy of terrestrial laser scanners", *INGEO 2004* and FIG Regional Central and

Eastern European Conference on Engineering Surveying, 11-13 November
Bratislava (Slovakia)

[13] <http://www.optech.ca/>

[14] <http://en.wikipedia.org/wiki/LIDAR>

[15] http://www.riegl.com/terrestrial_scanners/lms-z420i_/420i_all.htm

[16] http://en.wikipedia.org/wiki/3D_scanner#Time-of-flight

[17] <http://www.laser-ndt.com/profilometry.html>



Escola Politècnica Superior
de Castelldefels

UNIVERSITAT POLITÈCNICA DE CATALUNYA

ANNEX

TÍTULO: Development and analysis of Laser Scanner data

DEGREE: Technical Telecommunication Engineering

Speciality: Telematics

AUTHOR: Emma Riera Wilson

DIRECTOR: Michele Crosetto

SUPERVISOR: Jaume Piera Fernández

DATE: 05 of June of 2007

[1] Programme to calculate incidente angle:

```
# include <stdio.h>
# include <stdlib.h>
# include <math.h>
# include <cmath>
# include <malloc.h>

void main(void) {

    FILE *pdam,*pout;
    int aperto=0, aperto1=0,auxf,auxc,auxv,ncol,nvent,nlin,i,j,kk=0,ok1,ok2;
    double l1=0,l2=0,l3=0,po[3],v1[3],v2[3],v21[3],v11[3],norm[3];
    char inp_name[50], inp_name1[50];
    double x,y,z,a,b,c;
    double angle,cos;
    double **matx,**maty,**matz;

//Open input file
    while (aperto==0) {
        printf(" Inserte el nombre del fichero de entrada!\n");
        scanf("%s", inp_name);
        pdam=fopen(inp_name,"rb");
        if (pdam==NULL) {
            printf(" \n\tFichero no abierto pruebe de nuevo!\n");
        }
        else {
            aperto=1;
        }
    }

//Open output file
    while (aperto1==0) {
        printf(" Inserte el nombre del fichero de salida!\n");
        scanf("%s", inp_name1);
        pout=fopen(inp_name1,"w");
        if (pout==NULL) {
            printf(" \n\tFichero no abierto pruebe de nuevo!\n");
        }
        else {
            aperto1=1;
        }
    }

//Introduce number of lines and columns of the input file
    printf(" Inserire il numero di linee!\n");
    scanf("%d", &nlin);
    printf(" Inserire il numero di colonne!\n");
    scanf("%d", &ncol);
```

```
//Introduce the vector window
```

```
do
{
    printf(" Inerire el número de ventana de vector!\n");
    scanf("%d", &nvent);

    if((nvent>nlin/2)||((nvent>ncol/2))
    {
        if(nlin>=ncol)
        {
            printf("Valor de ventana demasiado grande máx %d
!\n",ncol/2);

            kk=1;
        }
        else
            kk=1;
            printf("Valor de ventana demasiado grande máx %d
!\n",nlin/2);
        }
        else
            kk=0;
    }while (kk==1);

    matx=(double **)malloc(nlin*sizeof(double *));
    for(j=0;j<nlin;j++)
    {
        matx[j]=(double *)malloc(ncol*sizeof(double));
    }

    maty=(double **)malloc(nlin*sizeof(double *));
    for(j=0;j<nlin;j++)
    {
        maty[j]=(double *)malloc(ncol*sizeof(double));
    }

    matz=(double **)malloc(nlin*sizeof(double *));
    for(j=0;j<nlin;j++)
    {
        matz[j]=(double *)malloc(ncol*sizeof(double));
    }

    auxf=0;
    while(auxf<nlin)
    {
        auxc=0;
        while (auxc<ncol)
        {
            fscanf(pdama,"%lf %lf %lf %d\n",&x,&y,&z,&i);
```

```

        matx[auxf][auxc]=x;
        maty[auxf][auxc]=y;
        matz[auxf][auxc]=z;
        auxc++;
    }
    auxf++;
}

```

```
auxf=0;
```

```

while(auxf<nlin)
{
    auxc=0;
    while(auxc<ncol)
    {
        kk=0;

```

//Create PO vector

```

po[0]=matx[auxf][auxc];
po[1]=maty[auxf][auxc];
po[2]=matz[auxf][auxc];

```

//If bad points (0,0,0) we force 0 angle

```

if((po[0]==0.000)&&(po[1]==0.000)&&(po[2]==0.000))
{
    angle=0;
    fprintf(pout,"%lf\n",angle);
    auxc++;
    kk=1;
}

```

angle //For the outline points we don't calculate vector, we force 0

```

if ((auxf==0)||auxf==nlin-1)
{
    for(auxc=0;auxc<ncol;auxc++)
    {
        angle=0;
        fprintf(pout,"%lf\n",angle);
    }
    kk=1;
}
if((auxc==0)||auxc==ncol-1)
{
    angle=0;
    fprintf(pout,"%lf\n",angle);
}

```

```

        auxc++;
        kk=1;
    }

    if(kk==0)
    {

        //Create vector 1
        ok1=0;
        if(nvent>(ncol-1)-auxc)
        {
            v1[0]=0;
            v1[1]=0;
            v1[2]=0;

            for(auxv=1;auxv<nvent;auxv++)
            {
                if(matx[auxf][auxc-auxv]!=0.0000)
                {
                    v11[0]=matx[auxf][auxc]-
                    v11[1]=maty[auxf][auxc]-
                    v11[2]=matz[auxf][auxc]-

                    v1[0]=(v1[0]+v11[0]);
                    v1[1]=(v1[1]+v11[1]);
                    v1[2]=(v1[2]+v11[2]);
                    ok1++;
                }
            }
        }
    }
    else
    {
        v1[0]=0;
        v1[1]=0;
        v1[2]=0;

        for(auxv=1;auxv<nvent;auxv++)
        {
            if(matx[auxf][auxc+auxv]!=0.0000)
            {
                v11[0]=matx[auxf][auxc]-
                v11[1]=maty[auxf][auxc]-
                v11[2]=matz[auxf][auxc]-

                v1[0]=(v1[0]+v11[0]);
                v1[1]=(v1[1]+v11[1]);
                v1[2]=(v1[2]+v11[2]);
                ok1++;
            }
        }
    }
}

```

```

v1[0]=(v1[0]+v11[0]);
v1[1]=(v1[1]+v11[1]);
v1[2]=(v1[2]+v11[2]);
ok1++;
    }
}

//Create vector 2

ok2=0;
if(nvent>(nlin-3)-auxf)
{
    v2[0]=0;
    v2[1]=0;
    v2[2]=0;

    for(auxv=1;auxv<=nvent;auxv++)
    {
        if(matx[auxf-auxv][auxc-auxv]!=0.0000)
        {
            v21[0]=matx[auxf][auxc]-
matx[auxf-auxv][auxc-auxv];
            v21[1]=maty[auxf][auxc]-
maty[auxf-auxv][auxc-auxv];
            v21[2]=matz[auxf][auxc]-
matz[auxf-auxv][auxc-auxv];

            v2[0]=(v2[0]+v21[0]);
            v2[1]=(v2[1]+v21[1]);
            v2[2]=(v2[2]+v21[2]);
            ok2++;
        }
    }
}
else
{
    v2[0]=0;
    v2[1]=0;
    v2[2]=0;

    for(auxv=1;auxv<=nvent;auxv++)
    {
        if(matx[auxf+auxv][auxc+auxv]!=0.0000)
        {
            v21[0]=matx[auxf][auxc]-
matx[auxf+auxv][auxc+auxv];

```

```

maty[auxf+auxv][auxc+auxv];
matz[auxf+auxv][auxc+auxv];

v21[1]=maty[auxf][auxc]-
v21[2]=matz[auxf][auxc]-

v2[0]=(v2[0]+v21[0]);
v2[1]=(v2[1]+v21[1]);
v2[2]=(v2[2]+v21[2]);
    }
}
}

if((ok1!=0)&&(ok2!=0))
{
    v1[0]=v1[0]/ok1;
    v1[1]=v1[1]/ok1;
    v1[2]=v1[2]/ok1;

    v2[0]=v2[0]/ok2;
    v2[1]=v2[1]/ok2;
    v2[2]=v2[2]/ok2;

    // "Producto vectorial" between vector 1 and
vector 2 to calculate normal vector
    norm[0]=v1[1]*v2[2]-v1[2]*v2[1];
    norm[1]=v1[2]*v2[0]-v1[0]*v2[2];
    norm[2]=v1[0]*v2[1]-v1[1]*v2[0];

    // "Producto escalar" between PO and Normal
vector, the incidente angle.

    a=po[0]*norm[0]+po[1]*norm[1]+po[2]*norm[2];

    b=sqrt((po[0]*po[0])+(po[1]*po[1])+(po[2]*po[2]));

    c=sqrt((norm[0]*norm[0])+(norm[1]*norm[1])+(norm[2]*norm[2]));

    cos=a/(b*c);
    angle=acos(cos);

    angle=angle*(180/3.1416);

    if(angle>90)
        angle=(180-angle);

    fprintf(pout,"%lf\n",angle);
    auxc++;
}

```

```

                                else
                                {
                                    angle=0;
                                    fprintf(pout,"%lf\n",angle);
                                    auxc++;
                                }
                            }
                    }
    auxf++;
}
printf(" Programa terminado!\n");

fclose(pdama);
fclose(pout);

return;

```

[2] Programme to calculate the Standard Deviation:

```

#include <stdio.h>
#include <stdlib.h>
#include <math.h>
#include <cmath>
#include <malloc.h>

void main(void) {

    FILE *pdama,*pout;
    int aperto=0, aperto1=0,auxf,auxc,ncol,nvent,ntot,nlin,i=0,j,f=0,kk,ja=0;
    char inp_name[50], inp_name1[50];
    double x,y,z,desv,a=1,b=0,med,suma,r=0;
    double **mat,*vect,**mat2;

//Open input file
    while (aperto==0) {
        printf(" Inserte el nombre del fichero de entrada!\n");
        scanf("%s", inp_name);
        pdama=fopen(inp_name,"rb");
        if (pdama==NULL) {
            printf(" \n\tFichero no abierto pruebe de nuevo!\n");
        }
        else {
            aperto=1;
        }
    }

//Open output file
    while (aperto1==0) {

```

```

        printf(" Inserte el nombre del fichero de salida!\n");
        scanf("%s", inp_name1);
        pout=fopen(inp_name1,"w");
    if (pout==NULL) {
        printf(" \n\tFichero no abierto pruebe de nuevo!\n");
    }
    else {
        aperto1=1;
    }
}
//Introduce number of lines and columns of the input file
printf(" Inserire il numero di linee!\n");
scanf("%d", &nlin);
printf(" Inserire il numero di colonne!\n");
scanf("%d", &ncol);
printf(" Inserire de la ventana!\n");
scanf("%d", &nvent);

mat=(double **)malloc(nlin*sizeof(double *));
for(j=0;j<nlin;j++)
{
    mat[j]=(double *)malloc(ncol*sizeof(double));
}

mat2=(double **)malloc(nlin*sizeof(double *));
for(j=0;j<nlin;j++)
{
    mat2[j]=(double *)malloc(ncol*sizeof(double));
}

vect=(double*)malloc((nlin*ncol)*sizeof(double));

auxf=0;
while(auxf<nlin)
{
    auxc=0;
    while (auxc<ncol)
    {
        fscanf(pdin,"%lf %lf %lf %d\n",&x,&y,&z,&i);

        r=sqrt((x*x)+(y*y)+(z*z));

        mat[auxf][auxc]=r;
        auxc++;
    }
    auxf++;
}

```

```

auxf=0;
while(auxf<nlin)
{
    auxc=0;
    while (auxc<ncol)
    {
        mat2[auxf][auxc]=0;
        auxc++;
    }
    auxf++;
}

auxf=nvent;
while(auxf<nlin-nvent)
{
    auxc=nvent;
    while(auxc<ncol-nvent)
    {
        if(mat[auxf][auxc]!=0.000)
        {
            ntot=nvent*nvent;

            med=0;
            ja=0;
            for(i=auxf-(nvent/2);i<nvent+(auxf-(nvent/2));i++)
            {
                for(j=auxc-(nvent/2);j<nvent+(auxc-
(nvent/2));j++)
                {
                    if(mat[i][j]!=0.000)
                    {
                        suma=mat[i][j];
                        med=med+suma;
                        ja++;
                    }
                }
            }
            med=med/ja;
            b=0;
            for(i=auxf-(nvent/2);i<nvent+(auxf-(nvent/2));i++)
            {
                for(j=auxc-(nvent/2);j<nvent+(auxc-
(nvent/2));j++)
                {
                    if(mat[i][j]!=0.000)
                    {
                        a=mat[i][j]-med;
                        a=a*a;

```

```

        b=b+a;
    }
}
}
desv=sqrt(b/ja);
    mat2[auxf][auxc]=desv;
}
auxc++;
}
auxf++;
}
auxf=0;
while(auxf<nlin)
{
    auxc=0;
    while (auxc<ncol)
    {
        fprintf(pout,"%lf\n",mat2[auxf][auxc]);
        auxc++;
    }
    auxf++;
}

/*auxf=0;
while(auxf<nlin)
{
    auxc=0;
    while (auxc<ncol)
    {
        fprintf(pout,"%lf\n",mat[auxf][auxc]);
        auxc++;
    }
    auxf++;
}*/

printf(" Programma terminato!\n");

fclose(pdin);
fclose(pout);

return;
}

```

